the exact wave function $\psi$ from the truncated representation for $g$, i.e., what is $V_{\text{eff}}$ if

$$(1-PgV_{\text{eff}})\psi=0$$

yields the exact wave function given in Eq. (51). Since we can write Eq. (52) as

$$\psi=PgV[1/(1-gQV)]\psi,$$

and using the calculable expression for $(1-gQV)^{-1}$ from Eq. (51), we obtain

$$\psi=PgV(1+G_0t)[1/(1+G_0Pt-G_0\tau_{12}G_0Qt)]\psi.$$

We then see that the effective operator which permits the use of a truncated representation for $g$, and yet yields the exact wave function, is

$$V_{\text{eff}}=t[1/(1+G_0Pt-G_0\tau_{12}G_0Qt)].$$

Neglecting the compact operator in the denominator of $V_{\text{eff}}$, we see that the wave function should again be approximately calculated from the lowest-order term:

$$\psi\simeq Pgt\psi.$$

We see that the $t$ operator of the residual interaction rather than the residual interaction potential is the one that appears in a convergent formulation of three-body shell-model calculations if only a finite set of basis states, $P\psi$, is used in the diagonalization of the residual interaction. Calculations that use an approximation for the $t$ matrix have recently been performed by Hodgson.[23] He finds that there is no definite improvement over a calculation that just employs the potential. Kuo and Brown[24] make use of the second Born term in the series for $t$, i.e., $t\simeq V+VG_0V$. They use core polarization states in the intermediate states of the term $VG_0V$. This implies that Kuo and Brown have included a structure in the core and have departed from a strict three-body shell-model interpretation of the problem. At any rate, they find the second Born term to be important.

[23] R. J. W. Hodgson, Phys. Rev. **156**, 1173 (1967).
[24] T. T. S. Kuo and G. E. Brown, Nucl. Phys. **85**, 40 (1966).

PHYSICAL REVIEW C VOLUME 1, NUMBER 3 MARCH 1970

# Nuclear Optical Model and Wave Properties: Barrier Penetration, Reflection, Absorption, and Resonance*

GEORGES MICHAUD†
*Department of Astronomy, California Institute of Technology, Pasadena, California 91109*
AND
LEONARD SCHERK‡ AND ERICH VOGT
*Physics Department, University of British Columbia, Vancouver, Canada*
(Received 11 July 1969)

A detailed study of the wave properties of the nuclear optical model is presented to elucidate the problem of barrier penetration by charged particles and to remove some of the mystique of optical-model calculations. The wave properties and the concomitant penetration are most straightforward for square wells, for which the resonance, reflection, and penetration are easily ascribed to separate factors. We show that the wave properties of more general diffuse-edge optical potentials achieve a similar simplicity by the construction of an equivalent square well (ESW) which has the same resonance, penetration, and absorption factors as the optical potential, but which differs in its reflection factor. A general construction of the ESW is given, and we apply it to the following problems: (1) the very narrow single-particle resonances of real optical potentials that occur at energies far below the Coulomb barrier, (2) the nuclear absorption cross sections in the presence of barriers, (3) the calculation of absorption cross sections at astrophysical energies (extreme barrier penetration) employing optical models fitted to data at higher energies, and (4) the value of the nuclear radius and sum-rule limits appropriate to the analysis of nuclear reactions. In some cases of extreme barrier penetration, the ESW fails to yield all the properties. For example, cases are described where the bulk of the absorption may attain in the distant "tail" of the imaginary term in the optical potential: The corresponding reaction rates can yield information about the behavior of the nucleus at distances much beyond the normal nuclear radius.

## 1. INTRODUCTION

THE behavior of most nuclear reactions at low energy—particularly those of interest for astrophysical systems—is dominated by Coulomb and angular-momentum barriers. Early treatments[1–3] of such reactions employed a simple picture: the "black-nucleus" or "black-box" picture. In this picture, a bombarding particle was viewed as passing through known Coulomb and angular-momentum barriers up to the nuclear radius. At the nuclear radius, it was ab-

* Work supported in part by a grant from the National Research Council of Canada and by grants from the National Science Foundation (Nos. GP. 9433 and GP. 9114) and the Office of Naval Research (No. Nonr-220-47).
† Present address: Département de Physique, Université de Montréal, Montréal, Canada.
‡ Present address: Department of Physics, University of Manitoba, Winnipeg, Canada.

[1] G. Breit and E. P. Wigner, Phys. Rev. **49**, 519 (1936); **49**, 642 (1936).
[2] H. A. Bethe, Rev. Mod. Phys. **9**, 69 (1937).
[3] V. W. Weisskopf and D. H. Ewing, Phys. Rev. **57**, 472 (1940); J. Blatt and V. W. Weisskopf, in *Theoretical Nuclear Physics* (John Wiley & Sons, Inc., New York, 1952).

sorbed by the "black box." This early picture was based on the short range and great strength of the nuclear forces.

During the last two decades, a microscopic model of nuclear structure has emerged which has changed our view of nuclear reactions and of barrier penetration. In spite of the short range and great strength of nuclear forces, it has been found that, in zero order, nuclei may be regarded as composed of neutrons and protons moving in orbits or shells and interacting with moderate potentials of finite range. The single-particle orbits or shells are those of an appropriate average potential well. The vestiges of such a single-particle picture remain in nuclear reactions. The neutrons and protons at low energy exhibit "giant" resonances[4,5] at the position of the single-particle levels of the average potential well. The resonances are broadened by nucleon-nucleon interaction, and, at high energy, the observed resonances resemble[6] those of the Ramsauer-Townsend effect in the electron bombardment of atoms.

The optical model of nuclear reactions accounts for the observed single-particle effects.[7] In the optical model, the interaction of a bombarding particle and a target nucleus is depicted in terms of a complex potential well. The real part of the potential refracts the incoming waves and the imaginary part absorbs them. The magnitude of cross sections is determined by the magnitude and shape of the optical potential. When Coulomb and angular-momentum barriers are present, the whole real potential of the system is the sum of the real part of the optical potential with the Coulomb potential and centripetal potential. Our aim in the present paper is to understand the formation of the compound nucleus in the presence of barriers and optical potentials. The absorption of waves by the imaginary part of the optical potential yields the compound-nucleus formation cross section, and the barriers dominate the behavior of the wave amplitudes in the absorbing region.

The formation of the compound nucleus has the following aspects, which are treated in subsequent sections of this paper:

(1) On the one hand, the optical model is a wave model and deals with the simple properties of wave penetration, refraction, reflection, and absorption. On the other hand, the optical potentials in common usage[7] have many phenomenological parameters. In order to understand how variations in the parameters affect cross sections, it is useful to describe the relationship between the parameters and the basic wave properties.

(2) Many of the reactions of interest in astrophysics occur at such low energy that they are rarely measured in the laboratory. In such cases, it is tempting to use an optical model which fits the more abundant data at higher energies to calculate the desired rates. Thus, the optical model serves as an extrapolation formula. Our analysis of the wave properties for the nuclear optical model allows us to understand the factors affecting the extrapolation.

(3) The early black-nucleus models are still frequently employed, particularly in astrophysical calculations where a very large number of reaction rates are required in a single calculation. The optical model is then often too cumbersome. It is therefore useful to know the relation between the cross section of the black-nucleus model and the corresponding cross sections of the optical model. We develop such relationships (Secs. 2, 3) as part of a general connection between diffuse-edge potentials and square wells.

(4) The theory of resonance reactions[8,9] is a very general and powerful framework for describing nuclear reactions. It has been successfully applied to the analysis of compound-nucleus resonances and to the cross sections of the statistical theory of nuclear reactions[10] in which averages are made over the compound-nucleus resonances. It provides a justification[11] for the description of the average cross sections by an optical-model potential. Nonetheless, the resonance theory has some of the undesirable features of the early black-box picture. For example, it relies explicitly on the use of a definite nuclear radius. Many of the common results of the resonance theory imply a square edge to the nuclear surface. In an earlier article,[12] one of us tried to show how the diffuse edge of the optical model could be accommodated in the general resonance theory for neutron reactions. That accommodation is extended in the present article (Sec. 4) to cover reactions involving Coulomb and angular-momentum barriers.

(5) In seeking to describe all nuclear reactions with the physical ideas of the optical potential, we need to reexamine the value of the nuclear radius. In the several decades during which the simple black-nucleus picture was employed to describe nuclear reactions, the

---

[4] H. H. Barschall, Phys. Rev. **86,** 431 (1952).

[5] See, for example, E. Almqvist, D. A. Bromley, J. Kuchner, and E. Vogt, in *Proceedings of the International Conference on Nuclear Structure, Kingston,* edited by D. A. Bromley and E. Vogt (University of Toronto Press, Toronto, Canada, 1960), p. 736.

[6] K. W. McVoy, Phys. Letters **17,** 42 (1965); Ann. Phys. (N.Y.) **43,** 91 (1967); see also J. M. Peterson, Phys. Rev. **125,** 955 (1962).

[7] H. Feshbach, C. E. Porter, and V. W. Weisskopf, Phys. Rev. **96,** 448 (1954); G. R. Satchler, in *International Nuclear Physics Conference, Gatlinberg,* edited by R. L. Becker *et al.* (Academic Press Inc., New York, 1967), p. 1.

[8] L. Eisenbud and E. P. Wigner, Proc. Natl. Acad. Sci. U.S. **27,** 281 (1941); E. P. Wigner, Phys. Rev. **70,** 15 (1946); **70,** 606 (1946); E. P. Wigner and L. Eisenbud, *ibid.* **72,** 29 (1947); T. Teichmann and E. P. Wigner, *ibid.* **87,** 123 (1952).

[9] A. M. Lane and D. Robson, Phys. Rev. **151,** 774 (1966).

[10] E. W. Vogt, in *Advances in Nuclear Physics,* edited by M. Baranger and E. W. Vogt (Plenum Press, Inc., New York, 1968), Vol. 1, 261.

[11] A. M. Lane, R. G. Thomas, and E. P. Wigner, Phys. Rev. **98,** 693 (1955).

[12] E. W. Vogt, Rev. Mod. Phys. **34,** 723 (1962).

usual choice of radius[3] was $R=1.4\ (A_1^{1/3}+A_2^{1/3})$ fm. Here, $A_1$ is the atomic weight of the target nucleus and $A_2$ that of the bombarding particle. The nuclear radius of the optical model is determined quite sensitively by the fits to the diffraction patterns of elastic scattering data, and it turns out to be much smaller, e.g., for nucleons, its value is approximately $R=1.25\ A_1^{1/3}$ fm. (In turn, the nuclear-charge radius as measured in elastic scattering is smaller still; the charge radius is $R=1.09\ A_1^{1/3}$ fm. The small difference of this radius from the normal radius of the nucleon-nucleus interaction lies in a number of effects, such as core polarization, which are beyond the scope of the present work.) There is an overwhelming amount of recent evidence suggesting that the smaller optical-model radius is the right one. Why was the earlier model wrong for several decades, particularly for reaction rates involving barriers where the cross section depends quite strongly on the choice of nuclear radius? Our elucidation of the optical potential suggests a fairly universal explanation. The early black-nucleus model implied a square nuclear edge and therefore had an unrealistic amount of wave reflection. It compensated for this attenuation of absorption by an appropriate increase in the nuclear radius.

Some preliminary results of our present investigation were described briefly in an earlier paper.[13] In our present paper, we try to give a complete account of all aspects of barrier penetration and the other wave properties within the scope of the optical model.

We begin our analysis (Sec. 2) with a comparison of the wave properties for diffuse-edge optical potentials and for similar square wells. The motive for bringing square wells into the analysis is twofold: First, the various cross sections for a square well can be written in the simple, familiar forms which make possible easy evaluation of the wave properties; second, for a square well, the basic wave properties are easily separated—barrier penetration occurs only beyond the square-well radius, reflection occurs at the square-well radius, and absorption and resonance within the square-well radius. The vehicle for the comparison (Sec. 2) is the absorption cross section. The comparison yields the dominant result of our work. It is found that for each diffuse-edge optical potential an equivalent square well can be defined uniquely. The cross sections of the diffuse-edge potential have the same simple form as those of its equivalent square well, with all the basic wave properties clearly separated. The only quantitative difference between the wave properties or cross sections of the two wells is shown to reside in the penetration and shift functions. The conventional square-well penetration and shift functions apply to the diffuse-edge well when they are multiplied by a reflection factor that depends on the surface thickness and reduced mass but not on the charge, energy, or angular momentum of the bombarding particle. Thus, the breakdown of the optical model into basic wave properties is achieved by means of equivalent square wells.

In Sec. 3, we carry out, for diffuse-edge optical potentials, the explicit construction of equivalent square wells and determine the corresponding reflection factors. In Sec. 4, we show that our analysis of wave properties based on the behavior of absorption cross sections (Sec. 2) also applies to purely real wells. The sharp resonances of a diffuse-edge real potential are given approximately in terms of the sharp resonances of the equivalent square well when the penetration factor and shift function of the latter are multiplied by a known reflection factor. In Sec. 5, we describe the behavior of general optical-model absorption cross sections and the circumstances under which there are some departures of the wave properties from those which may be dealt with in terms of equivalent square wells. In Sec. 6, we use our analysis of the basic wave properties of the optical potential to discuss the uncertainties in the conventional approach of astrophysics to the problem of extreme barrier penetration. In Sec. 7, we discuss a number of conclusions resulting from our work, including the place of the nuclear radius in the analysis of nuclear-reaction data.

The optical model has a firm foundation only for nucleon reactions, but it has also been found to be a very useful tool for describing heavy-ion reactions. It is more ambiguous for heavy ions—the resonance effects that are the strongest signature of the optical model are largely missing in this case—but it can accommodate the strong absorption and the diffuse nuclear edge that are of importance for heavy ions. Therefore, the optical model is perhaps the best simple model for dealing with heavy ions. Because of the mass and charge of the heavy ions, many of their basic wave properties are more complex than those of nucleons. Such reactions serve as a useful measure of the success of our approach. Although we shall seek to be general, most of our results will be illustrated with a particular case: the interaction of $\alpha$ particles with $^{32}S$. This example offers extreme barrier penetration and is typical of the astrophysical reaction rates to which our results might be applied.

Recently, a modified version of our methods was applied to an extreme case of barrier penetration—that of $\alpha$ decay in heavy nuclei.[14] Other applications are suggested in the following sections.

## 2. COMPARISON OF ABSORPTION CROSS SECTIONS OF DIFFUSE-EDGE OPTICAL POTENTIALS WITH THOSE OF SQUARE WELLS

In order to display the basic wave properties of diffuse-edge optical potentials, we shall compare them

[13] E. W. Vogt, G. J. Michaud, and H. Reeves, Phys. Letters **19**, 570 (1965).

[14] L. Scherk and E. W. Vogt, Can. J. Phys. **46**, 1119 (1968).

with square wells for which the wave properties are much more perspicuous. We begin by choosing and parametrizing those terms of the modern nuclear optical potential that are of interest to us.

For most scattering and absorption cross sections, the principal terms of the optical potential may be written

$$V(r) = -V_0\{1+\exp[(r-R_0)/a]\}^{-1}+iW(r). \quad (1)$$

Here, $V_0$ is the "depth" of the real part of the potential and has a value in the neighborhood of 50 MeV for nucleons and considerably more for heavy ions; $R_0$ is the nuclear radius whose value is about $1.25\ A^{1/3}$ fm for nucleons (where $A$ is the atomic weight of the target nucleus) and a slightly larger value for heavy ions; $a$ is the "surface thickness," which has a value of about 0.5 fm for nucleons and heavy ions, and $iW(r)$ is the imaginary term of the optical potential that leads to absorption. The imaginary term is usually chosen to have a shape either like that of the real term,

$$W(r) = -W_0\{1+\exp[(r-R_0)/a\}^{-1}, \quad (2)$$

which is called "volume absorption," or, alternatively, $W(r)$ is chosen to be larger in the region of the nuclear surface (this choice is called "surface absorption"). In the main part of our discussion, we will choose volume absorption in order to be specific. In Sec. 5, we will discuss in some detail the effect of the shape of $W(r)$ on the wave properties. The depth parameter $W_0$ typically has a value of 2–5 MeV for nucleons and somewhat larger values for heavy ions.

We have chosen to concentrate on the principal terms [Eq. (1)] of the optical potential because the other terms, which we neglect, do not modify our main results concerning wave properties. For example, the spin-orbit coupling term which is proportional to $\mathbf{l}\cdot\mathbf{s}$ (where $\mathbf{l}$ is the orbital angular momentum and $\mathbf{s}$ the spin) makes the optical-model phase shifts depend on both $\mathbf{l}$ and $\mathbf{j}$ ($\mathbf{j}=\mathbf{l}+\mathbf{s}$). Our treatment below, then, also must be carried out separately for each value of $l$ and $j$. Similarly, the isotopic-spin term, when important, makes it necessary to treat neutrons and protons on a common footing and leads to unusual cross-section contributions such as the "quasielastic" $(p, n)$ reactions. We could also accommodate such terms in our analysis. However, to clarify the wave properties we will ignore such refinements and deal only with the dominant terms of [Eq. (1)].

The optical potential of Eq. (1) [or the Woods-Saxon potential that the particular well shape of Eq. (1) is frequently called] will be shown to exhibit all of the basic wave properties such as barrier penetration, resonance, reflection, and absorption. The most straightforward manifestation of these properties occurs in the absorption cross section, and we therefore choose to begin our analysis with it.

For any reaction channel $\alpha$($\alpha$ labels the pair of reaction products and their state of excitation) described by an optical potential with phase shifts $\delta_{\alpha l}$, the absorption cross section is

$$\sigma_\alpha(\text{abs}) = (\pi/k_\alpha^2)\sum_l (2l+1)T_l(\alpha), \quad (3)$$

where

$$T_l(\alpha) \equiv 1-|\exp(2i\delta_{\alpha l})|^2. \quad (4)$$

The $T_l(\alpha)$ are called nuclear transmission functions. All of the properties of the absorption cross section are those of the transmission functions or, equivalently, those of the phase shifts. Therefore, the numerical calculation of the absorption cross section is straightforward—one needs merely to integrate the Schrödinger equation containing the optical potential to a large distance, where the decomposition of the wave function into incoming and outgoing waves yields the phase shift. But the numerical solution does not display the wave properties. To see these, we first examine the transmission functions of a complex square-well potential.

The transmission function of a complex square well of depth $-(V_0+iW_0)$ and radius $R_\alpha$ may be written

$$T_l(\alpha) = \frac{4P_l f_{\alpha l}^{\text{Im}}}{(1-S_l f_{\alpha l}^{\text{Re}}+P_l f_{\alpha l}^{\text{Im}})^2+(P_l f_{\alpha l}^{\text{Re}}+S_l f_{\alpha l}^{\text{Im}})^2}. \quad (5)$$

(For a derivation of this result and a detailed discussion of nuclear transmission functions see pp. 281–295 of Ref. 10.) Here $P_l$ is the usual penetration factor (used in nuclear-reaction studies)

$$P_l \equiv k_\alpha R_\alpha/[F_l^2(k_\alpha R_\alpha)+G_l^2(k_\alpha R_\alpha)], \quad (6)$$

where $F_l$ and $G_l$ are, respectively, the regular and irregular Coulomb wave functions of the channel $\alpha$. The $S_l$ are the usual shift functions of nuclear-reaction theory

$$S_l \equiv -b_{\alpha l}+\left\{\frac{rF_l dF_l/dr+rG_l dG_l/dr}{F_l^2+G_l^2}\right\}\Bigg|_{r=R_\alpha}, \quad (7)$$

in which the $b_{\alpha l}$ are boundary-condition numbers determined by the resonance properties of the well (see below). Finally, we have $f_{\alpha l}(\equiv f_{\alpha l}^{\text{Re}}+if_{\alpha l}^{\text{Im}})$ related in the following way to the logarithmic derivative of the wave function inside the square well $j_l(K_\alpha r)$:

$$f_{\alpha l} \equiv [r(dj_l/dr)/j_l|_{r=R_\alpha}-b_{\alpha l}]^{-1}. \quad (8)$$

The $f_{\alpha l}$ are complex numbers because the $K_\alpha$ are complex:

$$K_\alpha \equiv [(2m_\alpha/\hbar^2)(E+V_0+iW_0)]^{1/2}. \quad (9)$$

The quantities $f_{\alpha l}$ refer to the properties of the square well, while the quantities $P_l$ and $S_l$ refer to the external properties. The transmission functions [Eq. (5)] clearly exhibit absorption and barrier penetration in separate factors. The manifestation of resonance and reflection requires further analysis.

To exhibit the "resonances" of the transmission

functions of the square well, we take the real part of the potential and find the normal modes or resonances. The normal modes are solutions of the Schrödinger equation, which vanish at the origin and satisfy a suitable boundary condition at the square-well radius. If we write the solutions as $A_{pl}j_l(K_{pl}r)$, where $A_{pl}$ is a normalizing constant and $K_{pl}\equiv[2m_\alpha\hbar^{-2}(E_{pl}+V_0)]^{1/2}$ is the discrete value of the wave number for which the following boundary condition is satisfied:

$$r\,dj_l/dr=b_{\alpha l}j_l|_{r=R\alpha}. \tag{10}$$

The correct value of the boundary condition number $b_{\alpha l}$ is that which makes the shift function [Eq. (7)] vanish at the energy of interest.[12] The normal modes have single-particle energies:

$$E_{pl}=(\hbar^2/2m_\alpha)K_{pl}^2-V_0.$$

The $f_{\alpha l}$ are given quite generally in terms of spherical Bessel functions of complex arguments. Alternatively, we can give them in terms of the normal modes or resonances of the real part of the potential. By using the completeness of the resonances, we find

$$f_{\alpha l}^{\rm Im}\equiv\pi s_l=\sum_p\frac{\gamma_{lp}^2W_0}{(E_{lp}-E)^2+W_0^2}, \tag{11}$$

$$f_{\alpha l}^{\rm Re}=\sum_p\frac{(E_{lp}-E)\gamma_{lp}^2}{(E_{lp}-E)^2+W_0^2}=P\int_{-\infty}^{+\infty}\frac{s_l(E')dE'}{E'-E}, \tag{12}$$

where $P$ stands for the principal value of the improper integral and $\gamma_{lp}^2$ is the single-particle reduced width. If we choose the boundary condition number to be $b_{\alpha l}=-l$ (which would be correct for neutral particles in the low-energy limit), then $\gamma_{lp}^2=\hbar^2/m_\alpha R_\alpha^2$. The quantity $s_l$ defined by Eq. (11) is usually referred to as the strength function.

The nuclear strength function of Eq. (11) clearly exhibits a resonance structure. Using the corresponding value of $f_{\alpha l}^{\rm Im}$ in the transmission function [Eq. (5)] or in the absorption cross section [Eq. (3)] shows that these resonances also are expected to appear in the data. There is much evidence for them in low-energy nucleon absorption. For heavy ions, the values of $W_0$ are larger and the values of $E_p$ closer together, so that the data do not usually exhibit resonances.

The reflectivity of the square well can be traced to the penetration factor. For $l=0$ absorption of neutral particles, we have no Coulomb or angular-momentum barriers, and, therefore, the penetration factor [Eq. (6)] becomes $P_0=k_\alpha R_\alpha$. Near threshold, the strength function remains finite, but $P_0$ vanishes as $E^{1/2}$. This vanishing of $P_0$ can be traced to total reflection of the wave approaching the square-well radius from either side.

Having displayed absorption, barrier penetration, resonance, and reflection for square wells, we now seek to compare the corresponding quantities for diffuse-edge wells with our earlier results. It might appear reasonable to begin with a decomposition of the transmission function, as in Eq. (5). There is no feature of the decomposition of Eq. (5) that does not apply to an arbitrary well shape. We can always choose a matching radius, evaluate $P_l$ and $S_l$ for that radius (taking account of the modification of $P_l$ and $S_l$ by the tail of the complex potential), and evaluate the logarithmic derivative $f_{\alpha l}$ for the complex potential at that matching radius. Indeed, we can even decompose the logarithmic derivative of any well to exhibit the resonances as above. But how do we choose the matching radius? How do the penetration factors, strength functions, resonance energies, etc., depend on well properties? In our answers to these questions will reside our analysis of wave properties.

Before adapting our exposition to diffuse-edge potentials, we illustrate the decomposition of the transmission function [as in Eq. (5)] by the black-nucleus model, which is not a potential model at all. In this case it is assumed that there are only incoming waves for $r\leq R_\alpha$. Replacing $j_l$ by $e^{-iKr}$ in Eq. (8) and choosing $b_{\alpha l}=0$, we then have

$$f_{\alpha l}=i/KR_\alpha. \tag{13}$$

Using this value of $f_{\alpha l}$ in Eq. (5), we obtain the black-nucleus transmission functions

$$T_l(\alpha)=\frac{4P_l/KR_\alpha}{(1+P_l/KR_\alpha)^2+(S_l/KR_\alpha)^2} \tag{14}$$
$$=[4k/K/(1+kK)^2]\qquad\text{for } s\text{-wave neutrons.}$$

At low energies ($k\ll K$), all the transmission functions of the black-nucleus model (even those for $s$-wave neutrons) are very small because of wave reflection or wave penetration. At higher energies ($P\to kR_\alpha$, $k\to K$), the black-nucleus transmission functions approach their maximum value of unity.

Like the square-well model, the black nucleus has more reflection than a real nucleus. To understand the wave analysis of the black nucleus, we can compare it to a wave-guide problem[15] in classical electromagnetic theory. The bombarding wave approaches the nucleus, which is treated like a resonating cavity. The cavity is tuned so that waves propagate inward at the cavity entrance $R_\alpha$ with the given wave propagation number $K$. The tuning to accomplish this is not easily duplicated by a potential-well model. Just as it is difficult to build resonating cavities which are tuned in a certain way for all wavelengths, it is impossible to make optical-model potentials for which the black-nucleus conditions apply at all energies. The black-nucleus transmission functions completely lack the resonances of the square well: The square-well transmission functions oscillate about the black-nucleus trans-

[15] N. Austern, A. Prakash, and R. M. Drisko, Ann. Phys. (N.Y.) **39**, 253 (1966).

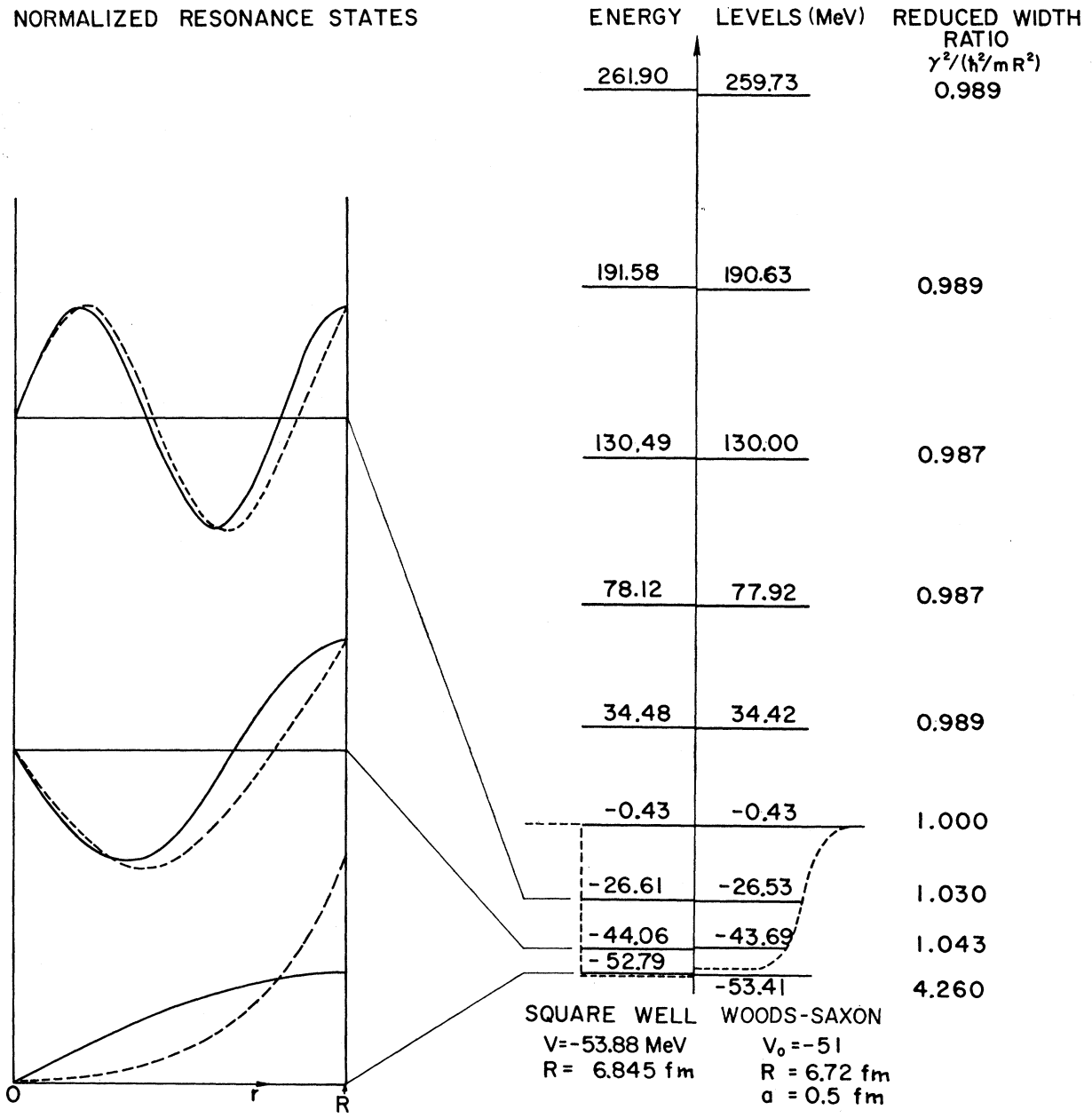


FIG. 1. Comparison of the low-laying resonant states of the square well and of the corresponding diffuse-edge well for $s$-wave neutrons. Once the depth and radius of the square well are adjusted so that both wells have a resonance with the same reduced width at $E=-0.43$ MeV, all other low-lying resonances in the two wells occur at very closely the same energy and with very nearly the same reduced width (expect for the reduced width of the resonance at $E=-53$ MeV). It is then possible for a square well to reproduce the interior properties of resonance of a diffuse well. The difference between the two wells is then contained only in the penetrability and shift functions.

mission function if we choose $K$ to have the same value for both. The two transmission functions have the same mean value. We show below that the transmission functions of a realistic nuclear optical potential have a larger mean value than both of the above models because the diffuse nuclear edge gives less reflection than a square edge. The black nucleus suffers the same unrealistic reflection because of the sudden change in the wave number at $R_\alpha$. Thus the black-nucleus model fails to a considerable degree in its main objective of optimizing nuclear absorption.

Much of the above wave analysis can be adapted at once to a realistic nuclear optical potential. For example, the decomposition of the transmission func-

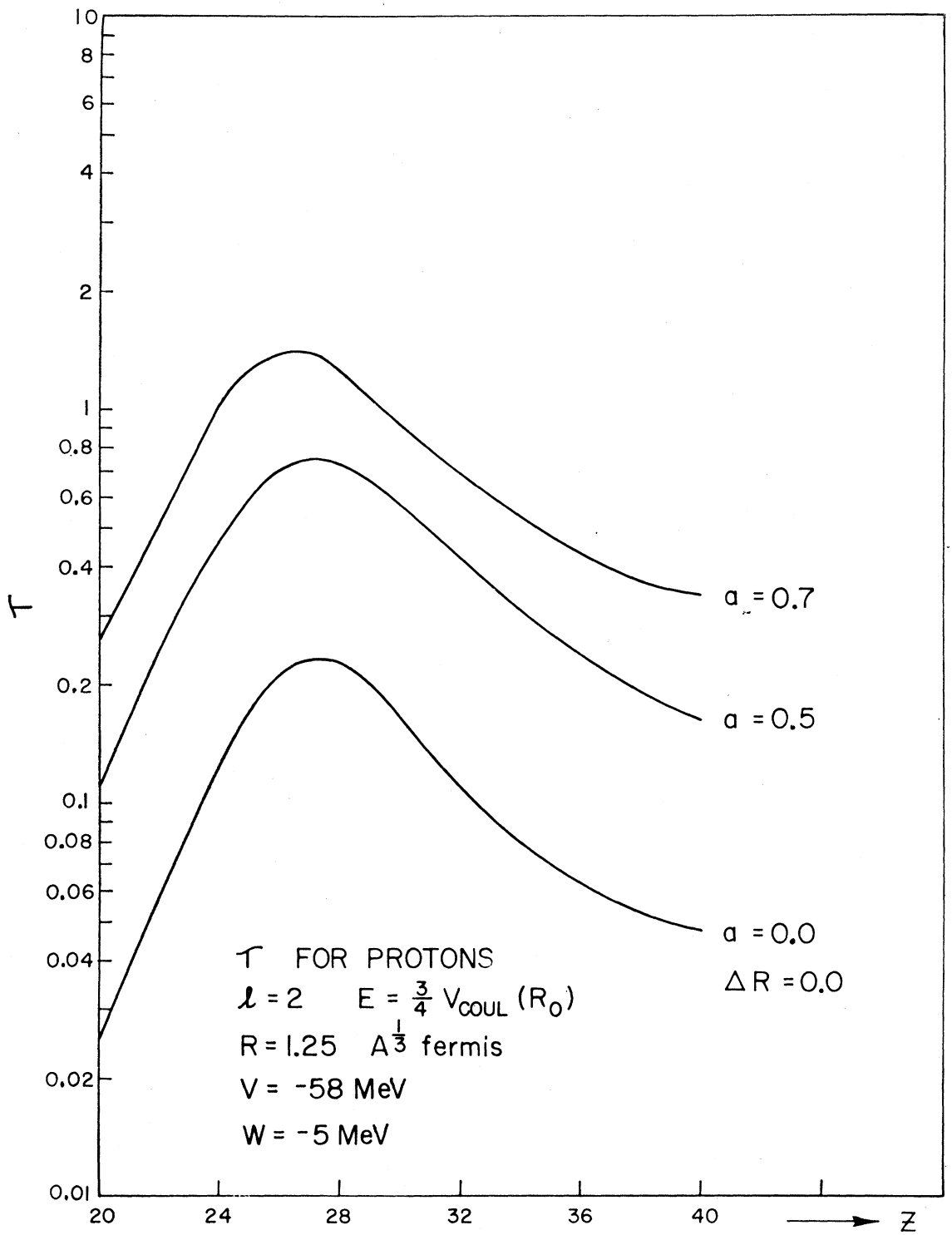


FIG. 2. Comparison of $\tau_2$ of protons for different values of the surface thickness $a$. Because the transmission functions are close to 1, it is necessary to compare $\tau_l$ to obtain the reflection factors. The $\tau_l$ are obtained from the transmission functions by using $T_l = \tau_l/(1+\tau_l/4)^2$. It is seen that by multiplying $\tau_2(a=0)$ by a factor $f(a)$, independent of energy, that one gets an excellent approximation to $\tau_2(a\neq 0)$. The interior of the two wells must then have very similar resonance properties. Only the penetrabilities vary. It then seems possible, as it was for neutrons, to replace a diffuse well by a square well.

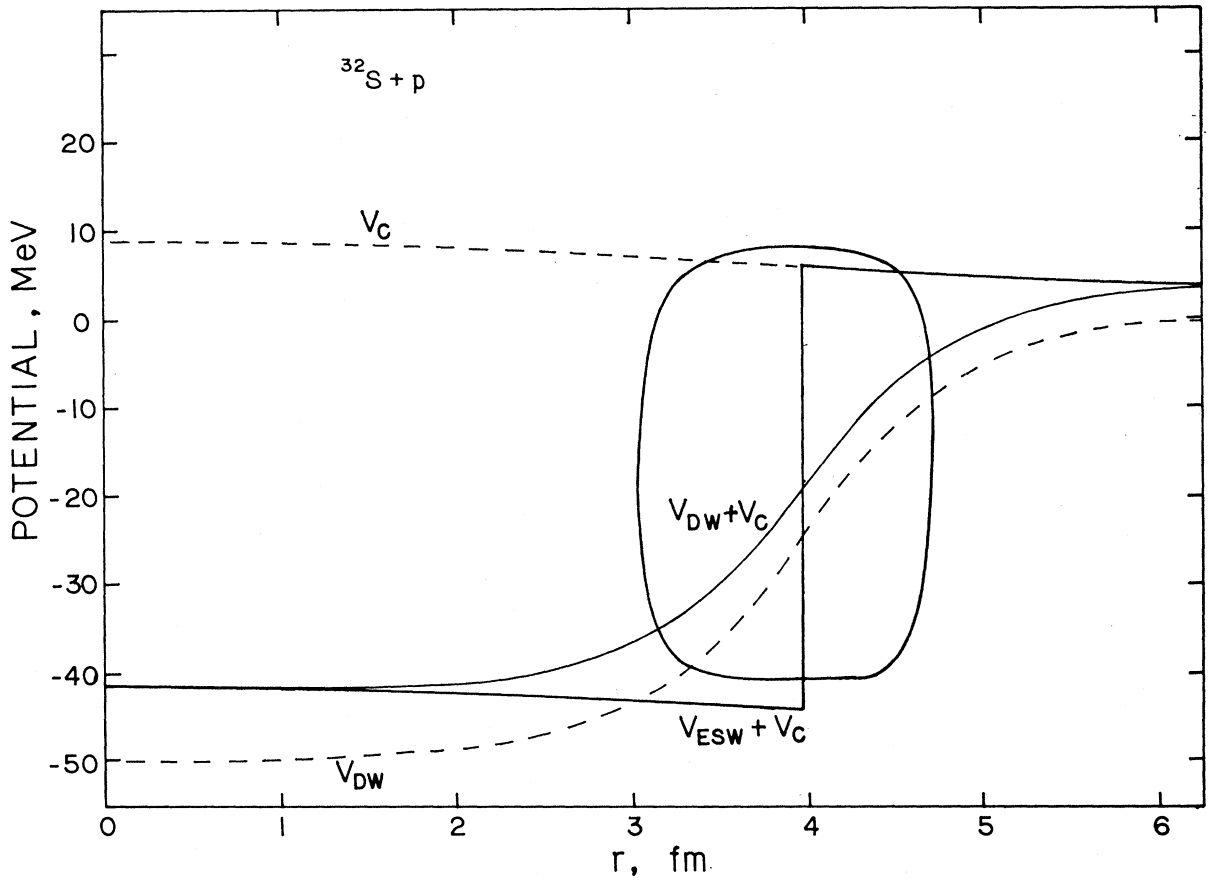


FIG. 3. The shape of the real potential for $s$-wave protons ($^{32}S+p$). The Coulomb potential ($V_c$) does add a radius-dependent term. However, its radius dependence is much weaker than the radius dependence of the nuclear potential ($V_{DW}$). In first approximation, the Coulomb field adds only a constant term that does not change the reflection properties of the two wells. Protons should behave like negative-energy neutrons. As is the case for neutrons, it should then be possible to find an equivalent square well ($V_{ESW}$) for changed particles. The difference between the two wells should again reside only in the reflection factor. This is vindicated by Fig. 2. In this example, the nuclear potential is chosen to have a Woods-Saxon shape with depth 50 MeV, radius 3.96 fm, and surface thickness 0.5 fm.

tion as in Eq. (5) still applies except that $P_l$, $S_l$, and $f_{\alpha l}$ are modified, and the choice of a matching radius at which these three quantities are to be evaluated is no longer obvious. The decomposition is valid for an arbitrary choice of matching radius, but, for our purposes, a well-defined choice will turn out to be useful. For an arbitrary radius we can find $P_l$ and $S_l$ from the logarithmic derivative of an outgoing wave $O_l$,

$$\frac{rdO_l/dr}{O_l} = \frac{rdF_l/dr+irdG_l/dr}{F_l+iG_l} \quad \text{(for large } r\text{)}$$
$$= S_l+b_{\alpha l}+iP_l \quad \text{(at the matching radius)} \quad (15)$$

simply by making the analytic continuation of the logarithmic derivative to the matching radius, as indicated. Similarly, $f_{\alpha l}$ is still given by Eq. (8) if, in Eq. (8), we replace $j_l$ by the appropriate regular wave function of the optical potential.

There are two important factors which narrow down the choice of matching radius in such a wave analysis. First, the nuclear surface of realistic potentials is still quite sharp [typically, $a/R_0$ in Eq. (1) has a value of 0.1]. Second, the resonance conditions themselves do not allow much freedom of choice. Considering the nucleus as a wave guide, we think of setting up normal modes or resonances. If we include in our definition of the wave guide part of the transmission channels that lead into it, then the resulting large—artificially large—dimension of the guide gives it unusual properties. Even when our wavelength is close to that of one of the artificial normal modes, the one-mode approximation is poor. In the nucleus, the one-level Breit-Wigner formula breaks down. We must choose the matching radius to lie reasonably close to $R_0$.

In an earlier work,[12] one of us showed that for $s$-wave neutrons there existed a very simple correspondence between the optical potential [Eq. (1)] and a square well of very nearly the same radius. Figure 1 shows the

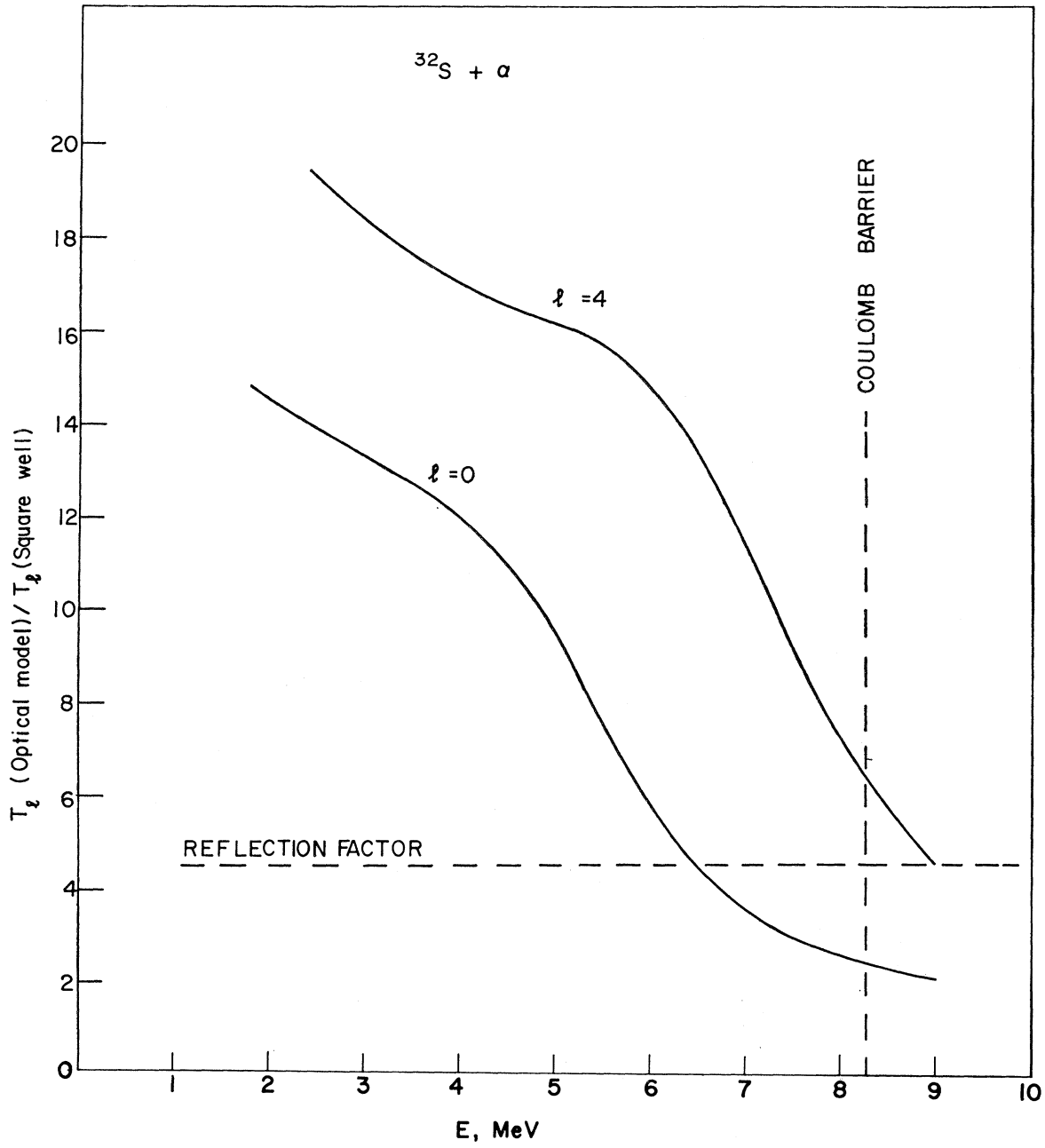


FIG. 4. Ratio of transmission functions of an optical potential suitable for $^4$He+$^{32}$S for two values of the surface thickness [$T_{l=0}(a=0.5\text{ fm})/T_{l=0}(a=0.0)$]. The two wells have the same $V_0$ and the same $R_0$. It seems either that the interior of the two wells show different resonance behavior or that different phenomena occur under the Coulomb barrier. It will be seen in the next sections that most of the energy variations of the ratio come from choosing two wells which do not have the same interior properties. Absorption in the barrier will be seen to become dominant only at very low energy ($E \leq 1$ MeV in this case).

important features of the correspondence. With the radii the same, the depth of the square well is adjusted so that the resonances near zero energy coincide for the two wells. With this choice it turns out that all of the resonance energies and all of the reduced widths of the two wells are the same. The two wells have exactly the same resonance properties. But the penetration functions and shift functions of the two wells are different. For the square well, the bracketed term of Eq. (7) is equal to $l$ at low energy, and, therefore, it is natural[12] to choose $b_{\alpha l}=l$ so that $S_l=0$. For the diffuse-edge well, one obtains $b_{\alpha l}$ by calculating the analytic continuation of the bracketed term and by choosing $b_{\alpha l}$ so that $S_l$ vanishes at low energy. The

correspondence of Fig. 1 is obtained with this choice. The penetration factors of the two wells differ by a constant factor $f$ which is nearly energy-independent. As shown first by Peaslee,[16] $f$ can be well approximated by

$$f=\pi Ka \coth \pi Ka, \tag{16}$$

which has a value of about 2.5 for the optical potentials in common use for nucleons. The factor $f$ accounts for the difference in reflection of the diffuse edge and square edge.

For $s$-wave neutrons, the correspondence between the optical potential and its equivalent square well extends to all cases, from real wells with narrow resonances to complex potentials with broad peaks in the transmission functions. In all cases, the square-well results apply also to diffuse wells if we merely multiply the square-well penetration function and shift function by the reflection factor $f$. Thus the whole wave analysis is established for the diffuse-edge wells. The correspondence of Fig. 1 was established for purely real wells. It extends to complex potentials too because we can include an imaginary term of square shape in the real logarithmic derivative simply by replacing $E$ by $E-iW_0$. Thus, Eqs. (11) and (12) apply to the diffuse-edge well also. The shape of the imaginary term is of little consequence because there is little reflection from the imaginary term (see, however, Sec. 5). When the transmission functions are much smaller than unity, they can be well approximated by

$$T \approx 4\pi P_l s_l f. \tag{17}$$

Here, they clearly show the common resonance and penetration factors of diffuse-edge and square wells and the reflection factor that distinguishes them.

The earlier analysis applied to $s$-wave neutrons, and it is not at all clear that in the presence of Coulomb barriers it is possible to decompose the transmission functions into wave properties in quite the same simple way. It turns out to be so for protons, as we show on Fig. 2. Here, transmission functions are shown well below the Coulomb barrier for $d$-wave protons. The radii of all the wells are the same, but the well depths are adjusted to make resonance energies coincide roughly. [The adjustment procedure is the following: If $V(r)$ is the real part of the optical potential, the

$$\int_0^\infty V(r) r\, dr$$

is taken to be constant for all potentials.] Although there is strong barrier penetration here, the relation between the various transmission functions is still that of Eq. (17).

It is not difficult to understand why the same prescription works for protons. Figure 3 shows the sum of the nuclear and Coulomb potential for the optical model and its equivalent square well. The point is that the Coulomb potential varies little in the surface region (encircled). Within the surface region, we might approximate the Coulomb potential as being constant. Then our reflection problem is exactly like that for $s$-wave neutrons of negative energy $E-B$, where $B$ is the barrier height. The earlier analysis would apply to this case.

It was surprising to us that the simple relationship between diffuse-edge wells and square wells appeared to break down completely for heavy ions. Figure 4 shows a similar ratio of transmission functions for $^{32}S+^{4}He$. The expected reflection factor in this case is $f=4.6$, according to Eq. (17), but the ratio of transmission functions is much larger. Moreover, it varies strongly with the energy and depends strongly on the orbital angular momentum.

There is a simple way in which the wave analysis for heavy ions is restored to the simplicity of that for nucleons. We explained that the matching radius for the optical potential had to be chosen to be reasonably close to $R_0$, the midpoint of the surface. But it does not need to be exactly $R_0$. In Sec. 3, we show that if we choose $R_\alpha=R_0+\Delta R$—with $\Delta R$ clearly defined and evaluated—we again get results as simple as those of Eq. (17). The role of $\Delta R$ is important for heavy ions and not for nucleons because the more massive heavy ions have wave functions which oscillate more rapidly (the wave guide commences earlier).

## 3. CONSTRUCTION OF EQUIVALENT SQUARE WELLS

For arbitrary optical potentials of the kind in Eq. (1), we wish to construct equivalent square wells (ESW) in order that we may display the basic wave properties of the potential. According to the approximate view of nuclear reactions depicted on Fig. 3, Coulomb barriers have no great effect on the reflection of a diffuse-edge optical potential, nor do angular-momentum barriers, as we shall show below. The problem of displaying the wave properties is then reduced to the case where we have $s$-wave neutral particles. According to earlier work,[12] the ESW for the case of $s$-wave neutral particles is independent of the energy of the particles or of the absorptive (imaginary) term in the optical potential. We can therefore construct the ESW using the scattering of zero-energy $s$-wave neutral particles in only the real part of the optical potential. The depth, radius, and reflection factor of the ESW constructed in this way are expected to apply to all the other, more complicated, cases as well. In later sections, we show to what extent the ESW is universal, and to what extent it enables us to display the basic wave properties for all cases.

Having reduced the construction of the ESW to the

[16] D. C. Peaslee, Nucl. Phys. **3**, 255 (1957).

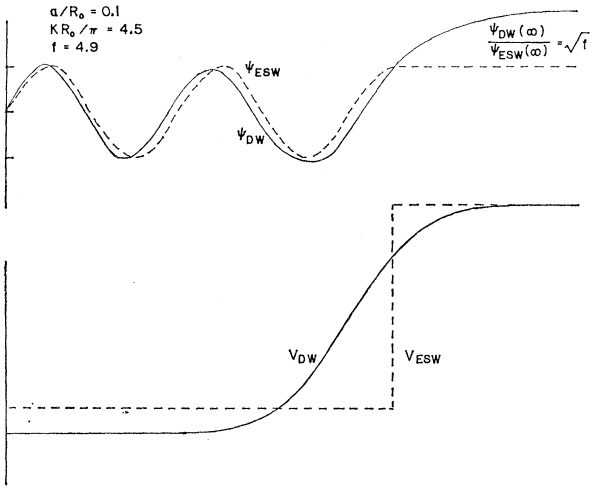


FIG. 5. A diffuse (solid) and a square (dashed) potential well and the corresponding $s$-wave zero-energy wave functions. The depth and radius of the square well were chosen so that it had a resonance at $E=0$ and so that the reduced width of that resonance would be the same as that of the diffuse well at the square-well radius. The interior properties of the two wells will then be the same as can be seen from Fig. 1. The wave function of the diffuse well continues to rise outside of the square-well radius. As discussed in the text, this can be related to the penetrability of the diffuse well and the differences between the square and diffuse potential can all be related to the ratio $[\psi_{DW}(\infty)/\psi_{DW}(R_{ESW})]^2$, whether we be studying narrow resonances far below the Coulomb barrier (Sec. 4) or the transmission functions of complex potentials (Sec. 5). The diffuse potential has been chosen to have a Woods-Saxon shape with interior wave number $K$, radius $R_0$, and surface thickness $a$.

case of zero-energy $s$-wave neutral particles of mass $m$ in the real part of the optical potential, we proceed, for all masses, in the way that was shown for neutrons in Fig. 1. Since the ESW is purely real, it has only two parameters, its depth $V_1$ and its radius $R_1$. On the other hand, the real part of the optical potential [Eq. (1)] has three parameters $V_0$, $R_0$, and $a$. We need two conditions to fix $V_1$ and $R_1$.

Both wells can have resonances at zero energy. For example, if we keep the depth of either well fixed and vary the radius (as we would do in proceeding through the Periodic Table), resonances occur at zero energy whenever the radial wave function has zero derivative beyond the well. Since the resonances greatly affect the scattering cross section, we must choose equivalent positions of the resonances in the two wells if we want the wells to have equivalent properties. Making the positions of the resonances coincide fixes one of the two parameters of the ESW.

A second condition is obtained from the widths of the scattering resonances. A conventional diffuse-edge potential has much larger widths than a square well, a fact which we associate with reflection. For each well, we can write the width $\Gamma_{nl}$ ($l=0$ in our case), where $n$ is the number of nodes of the $s$-wave resonant wave function, as a product of a penetration factor, and a reduced width

$$\Gamma_{n0}=2P_0\gamma_{n0}^2, \tag{18}$$

where the two factors are each evaluated at a suitable matching radius $R$. For the square well, it is natural and necessary to choose $R=R_1$, and for this choice we have $P_0=kR_1$ and $\gamma_{n0}^2=\hbar^2/mR_1^2$. For the diffuse-edge potential, we can easily exhibit a resonant wave function (as in Fig. 5) by varying $R_0$ until the wave function has zero derivative far beyond the well, but there is arbitrariness in the choice of the matching radius $R$. The width itself is independent of the choice of $R$, but the penetration factor and reduced width are not. At this stage we make a choice. (The choice is not entirely an arbitrary one any more than the choice of the matching radius in the $R$-matrix theory, for which the radius must be that of the actual nucleus if the resonance formulas are to have reasonable convergence properties.) We wish to associate the difference in widths (the reflection) with the difference in penetration of the two wells, and, therefore, we choose a matching radius $R$ such that the optical potential and its ESW have the same reduced widths at the common matching radius. Fixing the position and reduced width of the ESW determines $V_1$ and $R_1$.

The application of the above two conditions to the construction of the ESW is illustrated on Fig. 5. For a given optical potential, we fix $V_0$ and $a$, and then vary $R_0$ to find all of the resonances. We then have a discrete set of values of $R_0$ and the corresponding resonant wave functions (as shown in Fig. 5). Next, we begin with a square well with an initial choice of $R_1(\approx R_0)$, and fix $V_1$ so that we also get a zero-energy resonance in the square well that has the same number of nodes as the diffuse-edge resonance. For this initial choice, we compare reduced widths of both wells at the same matching radius $R=R_1$. If $\psi_{n0}(r)$ is the radial wave function of the resonance, the reduced width is given by[12]

$$\gamma_{n0}^2=(\hbar^2/2mR)[\psi_{n0}(R)]^2\left[\int_0^R\psi_{n0}^2(r)\,dr\right]^{-1}. \tag{19}$$

It is the square of the amplitude of the normalized wave function at the matching radius. If the two wells do not have the same reduced width for the initial choice of $R_1$, we vary $R_1$ (always adjusting $V_1$ so that the resonance positions of the two wells coincide exactly) until they do. In this way, we achieve a unique value of the depth and radius of the optical potential. This construction holds only for those values of $R_0$ which correspond to resonances, but we can interpolate the construction in between resonances.

The reflection factor is a direct result of the above construction of the ESW. It can be defined by

$$\Gamma_{n0}(\text{diffuse well})=f\Gamma_{n0}(\text{square well}). \tag{20}$$

Since the reduced widths of the two wells are the same, this yields

$$P_0(\text{diffuse well})=fP_0(\text{square well})=fKR_1. \tag{21}$$

The comparison of Eqs. (20) and (21) employed "natural" widths, not the observed widths of narrow resonances. We give a complete discussion in Sec. 4 of the relative values of observed and natural widths for various wells.

We can evaluate the diffuse-well penetration factor directly from Eq. (6) if we replace $F_l$ and $G_l$ by $\bar{F}_l$ and $\bar{G}_l$, where the latter are the radial wave functions of the optical potential that behave at large distance like usual radial wave functions ($F_l$ and $G_l$, respectively) in the absence of a potential. In our case, $F_0=\sin kr$ and $G_0=\cos kr$, so that, at zero energy, $F_0=0$ and $G_0=1$. Therefore, we find

$$f=[G_0(R)/\bar{G}_0(R)]^2=[\bar{G}_0(\infty)/\bar{G}_0(R)]^2$$
$$=[\psi_{\text{diff}}(\infty)/\psi_{\text{diff}}(R)]^2=[\psi_{\text{diff}}(\infty)/\psi_{\text{square}}(\infty)]^2, \tag{22}$$

since $\bar{G}_0$ is proportional to the diffuse-well resonant wave function of Fig. 5, and the resonant wave functions of the two wells are normalized to the same amplitude at the matching radius in Fig. 5. Then $f$ is just the square of the amplitude ratio of the resonant wave functions at large distance, as indicated in the figure.

If we remember the definition [Eq. (6)] of the penetration factor and employ the conventional definition of an incoming wave $I_l$ [$I_l\equiv F_l-iG_l$] we can give a similar physical meaning to the reflection factor that is valid at finite energy. The conventional penetration factor may be written

$$P_l=kR(F_l^2+G_l^2)^{-1}=kR(I_lI_l^*)^{-1}.$$

For a diffuse-edge well, we replace $I_l$ by its analytical continuation $\bar{I}_l$, yielding

$$\bar{P}_l=kR(\bar{I}_l\bar{I}_l^*)^{-1}=fkR(I_lI_l^*)^{-1},$$

where

$$f\equiv I_lI_l^*/\bar{I}_l\bar{I}_l^*.$$

The intensity of the incoming wave at large distance needed to yield a given intensity at the matching radius is $f$ times bigger for a square well than for a diffuse well. The reflection factor that we determine is related to wave reflection.

In the above construction of an ESW for a particle of mass $m$ and an arbitrary optical potential, only two of the four parameters ($V_0$, $R_0$, $a$, $m$) are independent. This can be seen from the radial equation with the optical potential $V$ [Eq. (1)].

$$-\frac{\hbar^2}{2m}\frac{d^2\psi}{dr^2}-\left[\frac{V_0}{1+\exp[(r-R_0)/a]}\right]\psi=E. \tag{23}$$

At zero energy, the right-hand side vanishes, and we can write Eq. (23) in terms of two dimensionless parameters

$$\frac{d^2\psi}{dx^2}=\frac{-(K_0R_0)^2}{1+\exp[(x-1)(R_0/a)]}\psi, \tag{24}$$

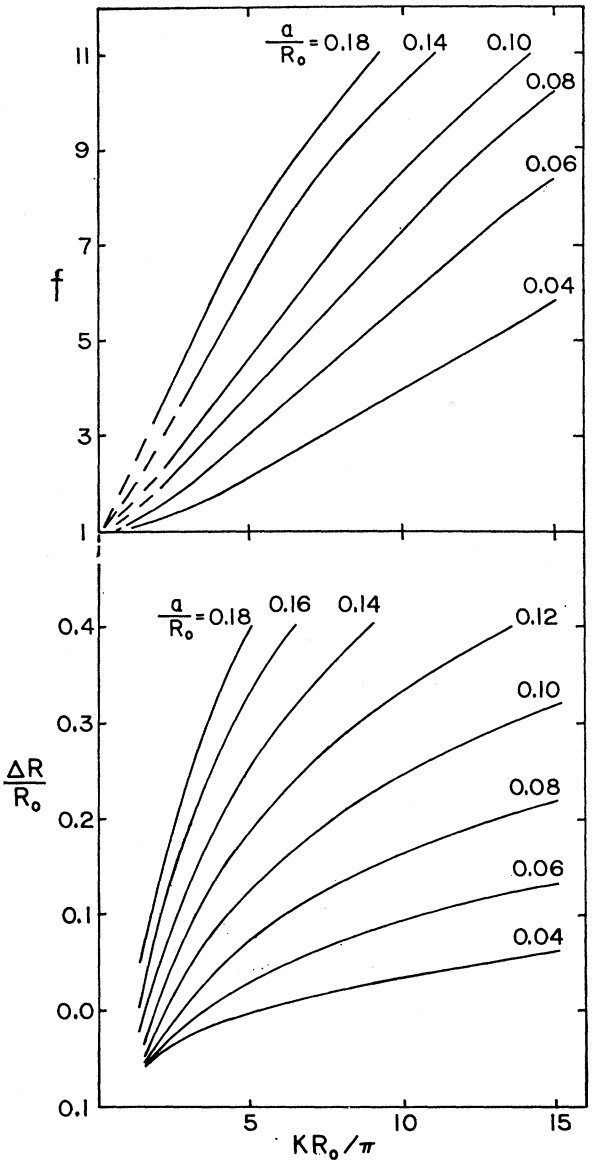


FIG. 6. The value of $\Delta R/R_0$ and of the reflection factor $f$, as a function of $a/R_0$ and $K\ R_0/\pi[=(2mV_0R_0^2/\hbar^2\pi^2)^{1/2}]$. This is the most frequently used section of Fig. 1 of Ref. 13. For a wider range of values, the reader is referred to Ref. 13. $\Delta R$ and $f$ allow one to determine the cross sections and the resonance width of diffuse wells, once those of square wells are known.

where

$$x=r/R_0, \tag{25}$$

$$K_0^2=2mV_0/\hbar^2. \tag{26}$$

Thus, $R_0$ determines only the scale of the abscissa in Fig. 5. The two important parameters are $K_0R_0$ and $R_0/a$. If we find $f$ and the ESW for all choices of these two parameters, we have covered all cases.

We carried out the construction of the ESW and the associated reflection factor for a large range of values of $K_0R_0$ and $a/R_0$. The depth of the ESW is not important

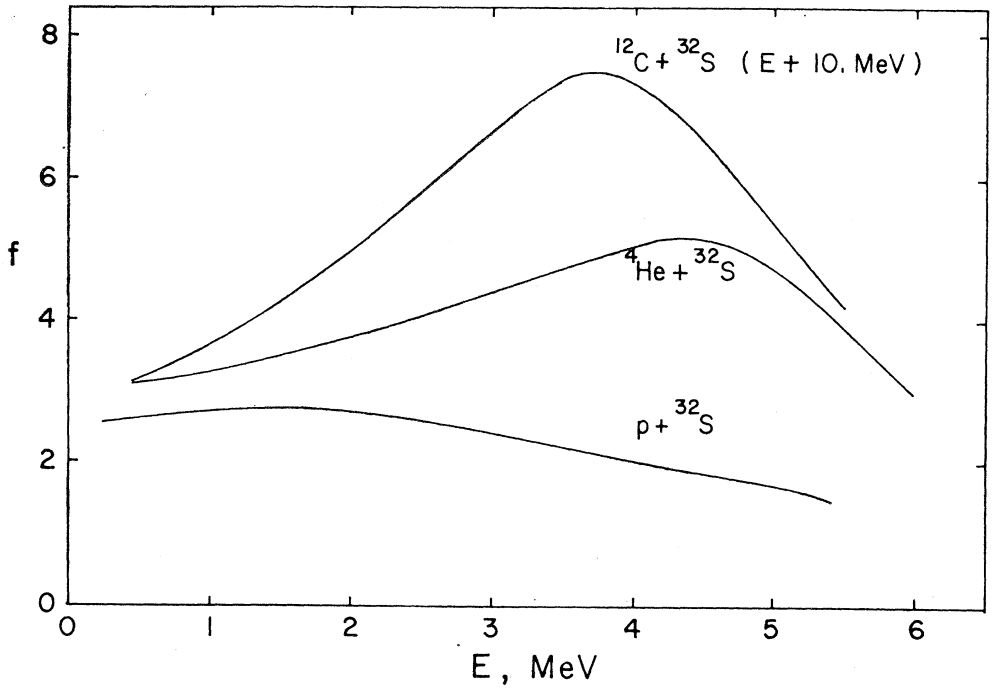


FIG. 7. The energy variation of the reflection factor was calculated from the ratio of the transmitted waves for a given incoming wave. We have made other calculations varying the Coulomb potential, but keeping the reduced mass and the nuclear potential the same. The reflection factor was then found to depend on $(B-E)$ only, where $B$ is the height of the barrier in the diffuse well. The reflection factor takes its maximum value at the energy $E=B_{max}$ where $B_{max}$ is the maximum value of the diffuse barrier. Letting the reflection factor vary with energy will, in some cases, improve the accuracy of the equivalent square-well model (not for the calculation of transmission functions, however). The energy variation of the reflection factor depends mainly on the reduced mass, and the figure may be used to estimate it, by interpolation, for cases not covered by our calculations. Note that for $^{12}C+^{32}S$ the energy scale is given by $E_{^{12}C+^{32}S}=E+10.0$ MeV.

in many applications, and it must always be adjusted to produce the resonant positions at the right energies (see Sec. 4) and is always found to be given very nearly by $V_1R_1^2\approx V_0R_0^2$. The ESW radius is usually important and differs appreciably from $R_0$. We present the results in terms of the radius difference $\Delta R/R_0$:

$$\Delta R/R_0=R_1/R_0-1, \tag{27}$$

which is also dimensionless. Figure 6 shows the values of $f$ and $\Delta R/R_0$ that we obtained from the zero-energy resonances and interpolations between resonances. Figure 6 is an enlargement of a small region of a corresponding map given by us in a preliminary report.[13] The enlargement given here contains the region of the map used in most applications.

Although our wave analysis of potential wells has taken the reflection factor to be energy-independent, the analysis of wave properties of potentials in terms of the equivalent square well can be generalized and improved by allowing $f$ to be energy-dependent.

In Fig. 7, we see the extent to which the reflection factor is independent of energy. The reflection factor was calculated by supposing an incoming wave at infinity and calculating the ratio

$$f=(I_{DW}/I_{ESW})^2,$$

where $I_{DW}$ and $I_{ESW}$ are evaluated at $R=0.1\ R_{ESW}$. To eliminate any possible effect of absorption in the barrier, we made our calculations by supposing that, for both the diffuse and square wells, absorption occurred only at $R=0$ and that the incoming wave was completely absorbed there. The reflection factor is then seen to be moderately dependent on energy. The energy dependence is also a function of the reduced mass and is larger for the heavier particles. We have also found that the energy dependence of the reflection factor was not a function of charge. It is the same within about 10%, whatever the Coulomb barrier, for a given reduced mass.

Before applying the ESW in some detail to obtain the basic wave properties of various problems, we give a simple example and discuss some special cases. For our standard example of $^{32}S+\alpha$, we can resolve the difficulties of Fig. 4. For a known optical potential with a diffuse edge, we now construct the ESW as above, with $\Delta R$ no longer zero but fixed by Fig. 6. The results are shown in Fig. 8. Now, the ratio of transmission functions at low energy is roughly equal to the reflection factor as expected from Eq. (17). There are corrections, however, the most important of which is absorption in the barrier. It largely cancels the energy

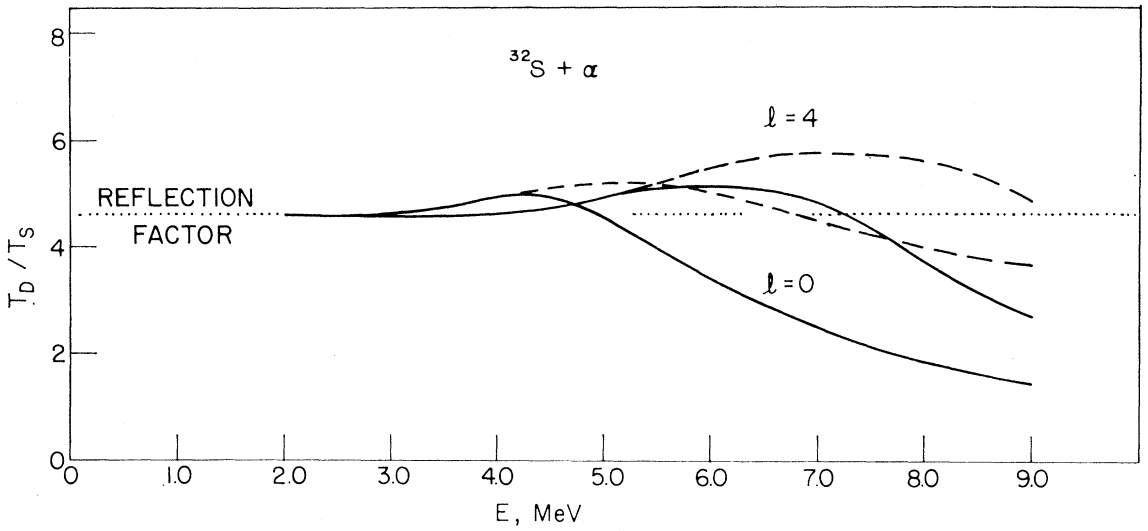


FIG. 8. The ratio of diffuse-edge optical-model transmission functions to equivalent square-well transmission functions as a function of the energy for $^{32}S+\alpha$. The diffuse potential is that of Fig. 4, and the equivalent square well has been calculated from Fig. 6 ($\Delta R=0.58$ fm). The reflection factor ($f=4.62$) is the ratio obtained at zero energy in the absence of Coulomb and angular-momentum barriers. It is seen that, if one chooses a correct value of $\Delta R$ for the ESW the observed reflection is insensitive to charge and centripetal barriers over a wide range of energies and is in close agreement with the reflection factor. In contrast, it was seen in Fig. 4, for a different square well ($\Delta R=0$), that the observed reflection depended strongly on all these factors. [The dashed lines give the corresponding ratios for $\tau_2=2\pi(\langle\Gamma_l\rangle/D)$ connected to the transmission functions by the approximate relation $T_l=\tau_l/(1+\frac{1}{4}\tau_l)^2$.]

variation of the reflection factor, so that the notion of a constant reflection factor becomes a good approximation. The corrections to the reflection factor will be further discussed in Sec. 5. The prescription for the ESW is obviously quite successful in this case.

For protons, $\alpha$ particles, and $^{12}C$ nuclei, we can apply Fig. 6 to conventional optical potentials. This is done in Fig. 9, which shows the value of $f$ and $\Delta R$ for these particles as a function of the bombarding nucleus. The results for $f$ are also compared in Fig. 9 to the approximate reflection factor [Eq. (16)] derived by Peaslee for $s$-wave neutrons.

## 4. SINGLE-PARTICLE RESONANCES FOR REAL POTENTIALS

The most straightforward case in which the ESW constructed in Sec. 3 can be applied to display the wave properties of optical potentials is for the elastic scattering resonances of real potential wells. The ESW was constructed from a matching of the resonances of neutral particles at zero energy. We now go to finite energy and also add Coulomb barriers, much as one might do in analyzing the scattering of $\alpha$ particles from light nuclei. In later sections, we go further still and add absorption to the picture (Sec. 5). The interest here is to show how well a zero-energy neutral-particle prescription applies to a realistic potential with barriers. The results will be useful in generalizing the formal many-channel theory of nuclear reactions (Sec. 7) to take into account the finite surface thickness of nuclei.

We begin with a real nuclear potential which might be suitable for $^{32}S+\alpha$. Choosing the Woods-Saxon form [Eq. (1)], we expect $V_0$ to be about 75 MeV, $R_0$ to be $1.25\,A^{1/3}+1.6$, and $a$ to be 0.5 fm. (This value of the radius is commonly used for optical-model analyses of $\alpha$-particle reactions. Its difference from 1.25 $(A_1^{1/3}+A_2^{1/3})$ or from the more fundamental radius of 1.09 $(A_1^{1/3}+A_2^{1/3})$, which is suggested by electron scattering data, is neither justified by the data nor important for our discussion.] We fix $a$ at 0.5 fm and $R_0$ at 5.5685 fm. The Coulomb barrier has a height of 8.3 MeV at $R_0$. Therefore, any $\alpha$-particle resonances at a few-MeV energy will be very narrow. For purposes of illustration, we chose a fixed resonance energy $E_{\rm res}=3.0$ MeV and varied $V_0$ in the vicinity of 75 MeV to obtain a single-particle $d$-wave resonance. Figure 10(a) shows such a resonant wave function obtained for $V_0=64.9$ MeV. At backward angles where Coulomb scattering is minimum, the scattering cross section is that of the Breit-Wigner formula

$$\frac{d\sigma}{d\Omega}=\frac{1}{4k^2}\frac{\Gamma_{n0}^2}{(E_{n0}-E-\Delta_{n0})^2+\frac{1}{4}\Gamma_{n0}^2}, \qquad (28)$$

where $\Delta_{n0}$ is the level shift. Figure 10(b) shows the scattering cross section near the energy of the resonant wave function of Fig. 10(a). The single-particle resonance of the optical-model well is 1.5 keV wide for this case.

In finding the single-particle resonance of an optical-model potential, we have completely specified the parameters of the potential. Therefore, we can at once

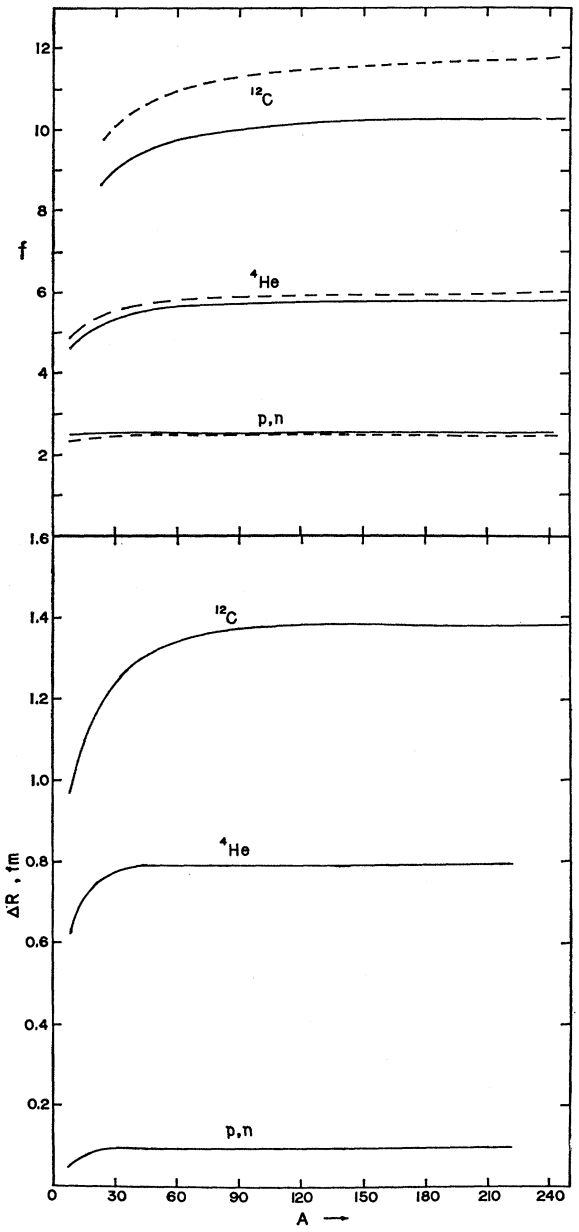


FIG. 9. $\Delta R$ and $f$ for $p$, $n$, $^4$He, and $^{12}$C incident on target nuclei of different masses. The diffuse potentials used had $R_0=1.25\ A_T^{1/3}$, $1.6+1.25\ A_T^{1/3}$, and $1.25\ (12^{1/3}+A_T^{1/3})$ and $V_0=50$, 75, and 100 MeV, for nucleons, $\alpha$ particles, and $^{12}$C, respectively, and $a=0.5$ fm in all cases. $\Delta R$ and $f$ were obtained from Fig. 6. We have also plotted with a dashed line (- - -) the approximation to $f$ obtained by Peaslee for $s$-wave neutrons [Eq. (16)]. The agreement is seen to be quite close for neutrons and protons.

use Fig. 6 to construct the ESW. In the present case the ESW has a radius of 6.25 fm and a depth $V_1=56.3$ MeV in order that it yield an $\alpha$-particle resonance with five nodes at 3.0 MeV. The ESW and its resonant wave function are shown in Fig. 10(a) and the corresponding scattering cross section in Fig. 10(b).

Clearly, both the optical potential and its ESW exhibit resonances. The resonance of the ESW is considerably narrower than that of the optical model, a fact which might be ascribed to reflection. We wish to enquire in some detail how the optical-model resonance properties can be described in terms of the ESW resonance properties after taking account of reflection. In order to do so, we need to factor the resonance widths into penetration factors and reduced widths, and we need to analyze the behavior of the level shift. In such a factorization, a part of the optical potential, the "tail" beyond the matching radius, modifies the shift and penetration factors from their conventional forms [Eqs. (7) and (6), respectively]. A rederivation of the Breit-Wigner formula (see Ref. 12, for example) shows that $P_l$ and $S_l$ still are given by Eqs. (6) and (7) if we replace $F_l$ and $G_l$ by their analytic continuations $\bar{F}_l$ and $\bar{G}_l$ to the maching radius. Denoting these by $\bar{P}_l$ and $\bar{S}_l$, we have

$$\Gamma_{n0}=2\bar{P}_0\gamma_{n0}^2, \tag{29}$$

$$\Delta_{n0}=-\bar{S}_0\gamma_{n0}^2. \tag{30}$$

Just as in Sec. 3, the matching radius of both wells for the factorization is the ESW radius $R_1=6.25$ fm. The reduced widths are obtained from the resonant wave functions by Eq. (19). In turn, the resonant wave function is found to be that wave function which behaves like the irregular solution $G_l$ far beyond the potential. The boundary condition number $b_l$ of the level shift function [Eq. (7)] is still to be chosen to make the left shift vanish at $E=E_{\rm res}$. However, both $\bar{P}_l$ and $\bar{S}_l$ are functions of the energy, and, therefore, we need to retain both $\Gamma_{n0}$ and $\Delta_{n0}$ in the Breit-Wigner formula.

There is no doubt about the validity of the one-level approximation in our case. The $^{32}$S+$\alpha$ resonances are about 10 MeV apart compared to the width of 1.5 keV.

The energy dependence of the level shift can be taken into account approximately by using a Taylor series for the shift about the energy and retaining only the lowest nonzero term

$$\Delta_{n0}=d\Delta_{n0}/dE\,|_{E=E_{n0}}(E-E_0). \tag{31}$$

Combining Eqs. (31) and (28), we can write the single-level resonance formula in the following way:

$$\frac{d\sigma}{d\Omega}\quad\frac{1}{4k^2}\,\frac{(\Gamma_{n0})^2}{(1-d\Delta_{n0}/dE)\,(E-E_{n0})^2+\frac{1}{4}\Gamma_{n0}^2}. \tag{32}$$

The effect of the energy dependence of the level shift on cross sections was first noted by Thomas[17] and is described in detail by Breit,[18] who has also computed those cases where approximation (31) fails. Thomas[17] has suggested that if Eq. (31) were a good approximation (as it should be for the extremely narrow res-

[17] R. G. Thomas, Phys. Rev. **81**, 148 (1951).
[18] G. Breit, in *Handbuch der Physik*, edited by S. Flugge (Springer-Verlag, Berlin, 1959), Vol. XLI, p. 1.

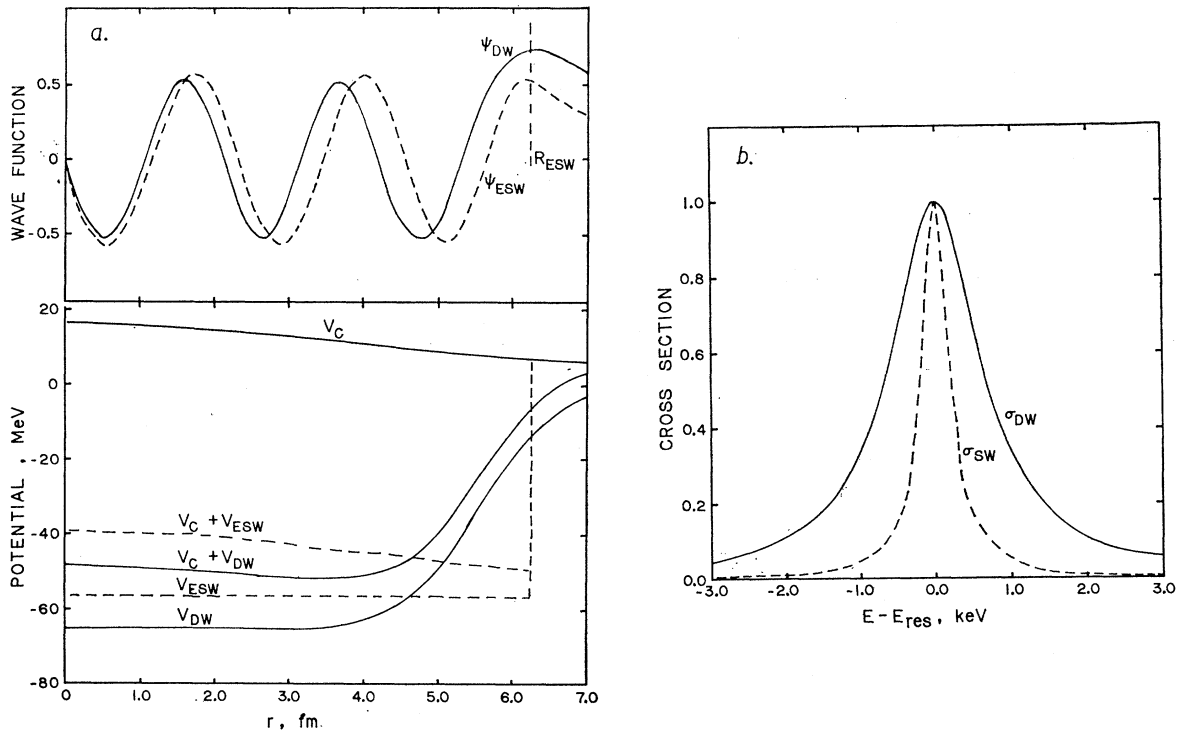


FIG. 10. The resonant $s$-wave functions [upper part of Fig. 10(a)] and the elastic scattering cross sections [Fig. 10(b)] for a diffuse potential (solid) appropriate to the reaction $^{32}S+\alpha$ and its ESW (dashed) [lower Fig. 10(a)]. The ratio (3.24) of the cross sections is simply related to the wave reflection factor (5.2) calculated in Sec. 3 through the energy dependence of the level shift. It is seen from the resonant wave functions that the reflection of the diffuse well is now distributed between the interior (resonant) and exterior (penetration) properties of the well. Nevertheless, the sum of the effects is what we would expect from the zero-energy barrier calculations. The diffuse well has a Woods-Saxon shape with depth $-64.9$ MeV, radius 5.5685 fm., and surface thickness 0.5 fm.; the ESW is found to have depth $-56.3$ MeV and radius 6.25 fm.

onances within a Coulomb barrier), the energy dependence of the level shifts be associated with the reduced widths

$$(\gamma_{n0}')^2 \equiv \gamma_{n0}^2/[1-d\Delta_{n0}/dE\,|_{E=E_{n0}}]. \tag{33}$$

In fact, he then found that the reduced widths of his calculation for a square well with Coulomb barrier were in close agreement with those appropriate to a square well without Coulomb barrier (i.e., $\hbar^2/mR^2$). With this association, we may naturally define the observed widths of the calculation

$$\Gamma_{n0}' \equiv 2P_0(\gamma_{n0}')^2 = \Gamma_{n0}/(1-d\Delta_{n0}/dE),$$

so that the single-level formula attains the simple form appropriate in the absence of level shifts

$$\frac{d\sigma}{d\Omega} = \frac{1}{4k^2}\frac{(\Gamma_{n0}')^2}{(E-E_{n0})^2+\frac{1}{4}(\Gamma_{n0}')^2}. \tag{34}$$

In comparing the resonance properties of the real optical potential and its ESW, there are a number of ratios that might be related to the reflection factor of 5.2 [or more precisely 4.4 at 3 MeV from Fig. (7)] found for our problem from Fig. 6. The ratios are

$$\begin{aligned}
&\text{(i)}\quad f' \equiv \Gamma_{\text{diff}}'/\Gamma_{\text{ESW}}' = f_P f_{\gamma^2} f_\Delta = 3.22,\\
&\text{(ii)}\quad f_{\gamma^2} \equiv (\gamma_{\text{diff}})^2/(\gamma_{\text{ESW}})^2 = 1.91,\\
&\text{(iii)}\quad f_P \equiv P_{\text{diff}}/P_{\text{ESW}} = 2.34,\\
&\text{(iv)}\quad f_\Delta \equiv [1-(d\Delta_{n0}^{\text{ESW}}/dE)\,|_{E=E_{n0}}]/\\
&\qquad\qquad [1-(d\Delta_{n0}^{\text{diff}}/dE)\,|_{E=E_{n0}}] = 0.727,\\
&\text{(v)}\quad f_{(\gamma')^2} \equiv (\gamma_{\text{diff}}')^2/(\gamma_{\text{ESW}}')^2 = 1.38,\\
&\text{(vi)}\quad f \equiv \Gamma_{\text{diff}}/\Gamma_{\text{ESW}} = 4.46,
\end{aligned} \tag{35}$$

where the numbers refer to our special case of $^{32}S+$ $^4He$ at 3 MeV. The first ratio $f'$ of the observed widths differs by an appreciable amount from the zero-energy zero-barrier result of 5.2, while the ratio $f$ of the one-body widths $\Gamma_{n0}$ is in moderately good agreement with these results and in excellent agreement with the one obtained at $E=3.0$ MeV [from Fig. (7)]. It must be remembered, however, that introduction of the surface effects into the channel widths will, in general, involve an adjustment for the energy dependence of the level shift ($f'=f_\Delta f$).

It is interesting to note that the factor $f'$ enters in a simple way into the level shift

$$d\Delta_{n0}^{\text{diff}}/dE\,|_{E=E_{n0}}=f'd\Delta_{n0}^{\text{ESW}}/dE\,|_{E=E_{n0}}. \quad (36)$$

To show this let

$$a_{nl}(R)\equiv\{(d/dE)[Ru_{nl}^{-1}(R)\,du_{nl}/dr]\}\,|_{E=E_{nl}},$$

$$a_{nl}^{\circ}(R)\equiv\{(d/dE)\,(R\bar{G}_l^{-1}(R)\,d\bar{G}_l/dr)\}\,|_{E=E_{nl}},$$

where $R$ is an arbitrary matching radius, $u_{nl}(r)$ is the normalized wave function appropriate to the $n$th $l$-wave resonance at energy $E_{nl}$ of the one-body potential, and $\bar{G}_l$ is the analytic continuation of the irregular $l$-wave Coulomb function. Since the one-level approximation applies, we have, near resonance, $a_{nl}(R)=\gamma_{nl}^{-2}(R)$. Moreover, suppressing the indices $(n, l)$, it is easily shown that $[a(R)/a(R_0)]=a^{\circ}(R)/a^{\circ}(R_0)$, where $R_0$ is the radius of the calculation. Since $a_{(\text{diff})}{}^{\circ}(R_\infty)=a_{(\text{ESW})}{}^{\circ}(R_\infty)$, we have [Eq. (36)]

$$f'\equiv\Gamma_{\text{diff}}'/\Gamma_{\text{ESW}}'$$

$$=\gamma_{\text{diff}}{}^2(R_\infty)/\gamma_{\text{ESW}}{}^2(R_\infty)$$

$$=[\gamma_{\text{diff}}{}^2(R_0)/\gamma_{\text{ESW}}{}^2(R_0)][a_{\text{diff}}{}^{\circ}(R_0)/a_{\text{ESW}}{}^{\circ}(R_0)].$$

In fact, in the example of $^{32}\text{S}+\alpha$, the ratio of Eq. (36) turns out to be 3.26 while $f'$ has the value 3.22 of Eq. (35). The observed widths of the real diffuse-edge potential can then again be stated in terms of the parameters of its ESW

$$\Gamma_{\text{diff}}'=f\Gamma_{\text{ESW}}\Big/\left(1-f'\frac{d\Delta_{n0}^{\text{ESW}}}{dE}\right)\Bigg|_{E=E_{n0}} \quad (37)$$

by the positive solution of the simple quadratic equation

$$cf'^2-f'+(f-cf)=0,$$

where

$$c\equiv d\Delta_{n0}^{\text{ESW}}/dE\,|_{E=E_{n0}}. \quad (38)$$

Hence, we may state the widths [Eq. (37)] of the diffuse-well entirely in terms of the parameters of the square interaction and of the standard reflection factor $f$, obtained from the zero-energy zero-barrier case. [In an earlier calculation on $\alpha$-decay rates in heavy nuclei,[14] it was of heuristic value to define an ESW in a slightly different manner. To have chosen the ESW to have the parameters suggested in Sec. 3 would have yielded a reflection factor consistent with that found for neutral particles at zero energy, but (as we have shown in the present analysis) this reflection would have been divided between the interior aspects (reduced widths) and exterior aspects (penetrabilities) of the $\alpha$-decay problem. Our point was that previous authors had treated the penetrabilities correctly but had not accounted for the enhancement of the wave function in the nuclear surface effected by the diffuse nuclear edge. In fact, this enhancement explained the anomalous radii which had plagued earlier $\alpha$-decay rate calculations (which had generally taken the nuclear interior to be square). This was most easily displayed by constructing an ESW from first principles, that is, in the manner of Sec. 3: The radius and depth of the ESW were chosen so that the resonant wave functions of the diffuse and square well had the same number of nodes and the same amplitude at the ESW radius. The radius of this ESW was found to be considerably larger than that of the diffuse-well, explaining much of the anomaly in the previous calculations.]

## 5. COMPLEX OPTICAL POTENTIALS

We wish to extend our treatment of barrier penetration to the case of complex optical potentials. As in the case of barriers and real optical potentials (Sec. 4), the combination of barriers with complex potentials will be shown to exhibit many of the simple wave properties present where there are no barriers at all. Again, there are some straightforward modifications of the simple wave properties brought about by the introduction of barriers. As in our earlier discussion, we shall use the example $^{32}\text{S}+\alpha$ to illustrate the main points.

In the absence of barriers, the addition of an imaginary term to a real optical-model potential introduces absorption, it broadens the wave resonances, but it has an almost negligible effect on wave reflection.[12] The imaginary term is normally chosen, both for nucleons and heavy ions, to have a small magnitude compared to the real term. Therefore, the reflection from the imaginary term is small—indeed, the absorption and scattering cross section of a complex potential well are relatively insensitive to the shape of the imaginary term. For the same reasons, we expect the same kind of changes when, in the presence of barriers, we add an imaginary term to the optical potential. Absorption enters the picture, the resonances broaden, but the wave reflection should remain relatively unchanged.

At low energy, the wave reflection properties manifest themselves most directly in nuclear transmission functions. In Fig. 8, we showed a straightforward application of the zero-energy zero-barrier results to the transmission functions for $^{32}\text{S}+\alpha$. The success of the model of Sec. 3 appears to be greater for the transmission functions than for the widths discussed in Sec. 4. In order to elucidate to what extent the ratio of the transmission functions should be related to the reflection factor, we have calculated that ratio over a wide range of energies and for reactions involving widely different Coulomb barriers. To analyze those results, we examine the effect of introducing a square and then a diffuse absorbing part to the potential. We find that the reflection properties are negligibly affected by the presence of an imaginary potential, but that, if the absorbing potential has a diffuse edge, an important fraction of the absorption may take place much beyond the normal nuclear radius.

The nuclear transmission functions are calculated exactly by means of Eq. (4) from the complex phase shifts of complex potentials. In turn, the phase shifts are calculated directly from numerical integration of the wave equation to a point well beyond the nuclear radius, where the numerical solution is matched on to standard Coulomb wave functions. The exact transmission functions found in this way can have their wave properties exhibited as in Sec. 2. If we adopt the form (5) for the transmission function, with the appropriate modifications made for diffuse-edge potentials as discussed in Sec. 2, a simple choice of the boundary condition numbers $b_l$ is one which makes the shift function $S_l$ vanish. With this choice we have

$$T_l=\tau_l/(1+\tau_l/4)^2, \tag{39}$$

where $\tau_l$ is defined by

$$\tau_l=4\pi f P_l s_l. \tag{40}$$

Here, $P_l$ is the penetration function, $s_l$ the strength function, and $f$ the reflection factor discussed in Sec. 2.

The result [Eq. (39)] for the form of the transmission function explains the results of Fig. 8, both the simple ratio of transmission functions at low energy and also the corrections pertaining at higher energy. At low energy, far below the barrier, $\tau_l/4$ is much smaller than unit, so that $T_l\approx\tau_l$. The ratio of the diffuse-edge transmission function to that of the ESW then should be equal to the reflection factor. This is found to be so in Fig. 8. At energies approaching the top of the Coulomb barrier, it is not the transmission functions themselves but rather the ratio of $\tau_l$ that should equal $f$. Again, this is found to be verified by Fig. 8. These results and many other similar results that we obtained but cannot show here justify our claim that the ESW should be independent of both the Coulomb and the angular-momentum barriers. A comparison of Figs. 5 and 8 shows the importance of $\Delta R$ in the choice of the ESW for heavy-ion reactions.

Although the dominant wave properties of complex wells are given in the discussion above, there are some minor and some major corrections in certain cases. Two minor corrections (each less than 10% in our standard $^{32}S+\alpha$ reaction) arise from resonance effects and from reflection by the imaginary part of the potential. The former of these manifests itself in a slight energy dependence of the strength function when Eq. (39) is fitted to calculated transmission functions. Although minor for most heavy-ion reactions the resonance corrections can become very large if the value of $W_0$, the depth of the imaginary term in the potential, becomes smaller than the single-particle level-spacing in the real part of the well. The reflection induced by $W_0$ is small in all cases of practical interest. It can be shown that a rough estimate of this effect is to replace $V_0$ by $(V_0^2+W_0^2)^{1/2}$ in Peaslee's formula [Eq. (16)] for the reflection factor.

A major correction to optical-model analyses concerns absorption deep within the barrier, which occurs at energies very far below the Coulomb barrier. It follows from an application of Green's theorem to the wave equation[19] that the transmission function $T_l$ is exactly proportional to the integral of the imaginary part of the potential

$$T_l=c\int_0^\infty W(r)\psi_l\psi_l^*dr, \tag{41}$$

where $c$ is a constant and $\psi_l$ is the radial wave function, obtained by numerical integration of the wave equation with the optical potential. In certain cases, important contributions to the integral of Eq. (41) occur well beyond the normal nuclear radius. The point is straightforward. Within the barrier, the wave function increases exponentially:

$$\psi_l\propto e^{Kr}, \tag{42}$$

$$K\equiv[(2m/\hbar^2)(B-E)]^{1/2}, \tag{43}$$

where $B$ is the height of the barrier and $E$ is the energy. The absorbing potential [Eq. (2)] for $r-R_0\gg a$ falls off as $e^{-r/a}$. Therefore, the contribution to the absorption from the region within the barrier becomes important at energies such that $2K$ approaches the value of $a^{-1}$. If we take a standard value of 0.5 fm for $a$, we find $2Ka=0.23\,[m(B\text{-}E)]^{1/2}$ where $m$ is the reduced mass (in units of the proton mass) and $(B\text{-}E)$ is in MeV.

The absorption within the barrier is of great importance for many heavy-ion reactions. Its magnitude can be estimated by means of Eq. (41). In our standard case of $^{32}S+\alpha$ at 3 MeV, 16% of the absorption occurs beyond the ESW radius. This absorption does not obey the normal rules: It is not subject to a correction due to reflection, and it tends to increase linearly with the value of $W_0$. It is important to remember that the effect on the transmission functions of absorption in the barrier is opposite to that of the energy dependence of the reflection factor. As we go down in energy from the top of the barrier, the absorption in the barrier tends to increase $T_l$, while the energy dependence of $f$ decreases $T_l$. For many commonly used optical potentials, the two effects nearly cancel. More importantly, it suggests that some astrophysical reaction rates will be dominated by the tail of the imaginary part of the optical potential. In such cases the optical model loses its utility in extrapolating from measurements at high energies to astrophysical rates far below the barrier. Conversely, it raises the prospect that absorption cross-section measurements at low energies can provide important information about nuclear densities far beyond the nuclear radius.

An extreme example of barrier absorption is shown in

[19] M. A. Preston, in *Physics of the Nucleus* (Addison Wesley Publishing Co. Inc., Reading, Mass., 1962).

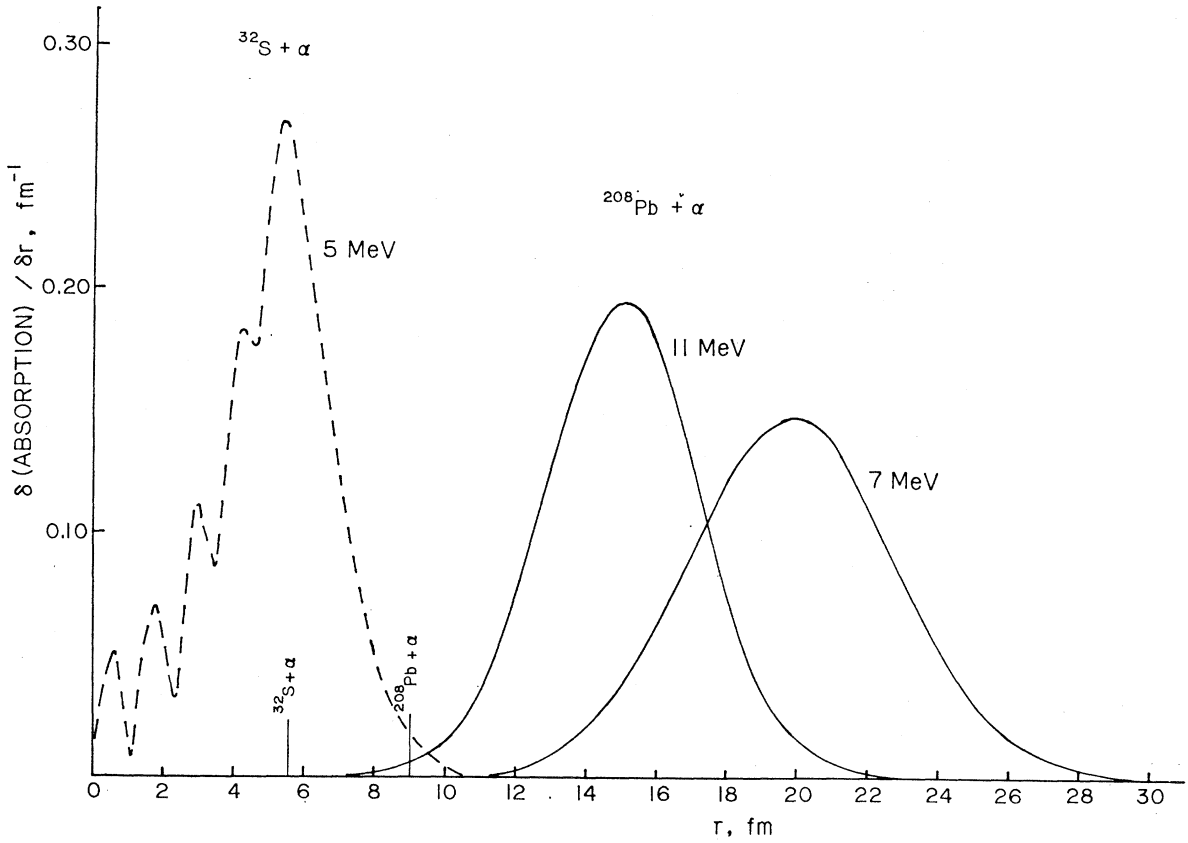


FIG. 11. Fraction of the absorption as a function of radius for diffuse potentials with parameters appropriate to the reactions $^{208}$Pb+$\alpha$(solid) and $^{32}$S+$\alpha$(dashed). The radii used for the Woods-Saxon wells are indicated by vertical lines. The relative amount of absorption in the barrier is seen to be greatly increased by the extreme barriers associated with heavy nuclei. In fact, at low energies ($\lesssim$7 MeV), all absorption occurs in the barrier if we use a conventional Woods-Saxon shape for the imaginary potential (with a radius $R_0$ of 5.568 fm for $^{32}$S+$\alpha$ and of 8.8 fm for $^{208}$Pb+$\alpha$). Hence, the nature of the imaginary potential in the barrier region is critical in describing absorption cross sections. If the absorption described by the figure is, in fact, physical, the equivalent square-well model would fail badly since most particles would be absorbed before reaching the nuclear surface.

Fig. 11 for the $^{208}$Pb+$\alpha$ reaction at an energy of 8 MeV, appropriate to the inverse of the $\alpha$ decay of $^{212}$Po. Here the absorption is important at twice the nuclear radius, at values of $r$ comparable to $R_0+15a$. Many optical-model programs in current use would throw away the barrier absorption because they match the numerically integrated wave functions to Coulomb functions at too small a radius.

## 6. USE OF OPTICAL MODEL IN ASTROPHYSICS

Current efforts by astrophysicists to determine the late stages of evolution of the stars and to determine the early history of the universe according to the "Big Bang" theory require the knowledge of a large number of charged-particle reaction rates.

According to the Big Bang theory,[20] matter would have emerged from thermodynamic equilibrium at very high temperatures ($T\gtrsim10^{10}$ °K) and would have cooled down as it expanded. The amount of nuclear transmutations occurring as the matter expanded, the energy release during that time, and the temperature at which the nuclear reaction rates become too slow to allow any more nuclear reactions to occur depend sensitively on charged-particle reaction rates. On the other hand, once the stars, in their deep interiors, have burned all their hydrogen and all their helium, $^{12}$C and $^{16}$O are expected to burn until, after their exhaustion, $^{28}$Si decomposes itself into $\alpha$ particles which, adding themselves to $^{28}$Si seed nuclei, form the iron peak.[21]

The $^{12}$C+$^{12}$C and the $^{16}$O+$^{16}$O reactions have been

[20] R. V. Wagoner, W. A. Fowler, and F. Hoyle, Astrophys. J. **148,** 3 (1967).

[21] J. W. Truran, A. G. W. Cameron, and A. Gilbert, Can. J. Phys. **44,** 563 (1966); D. Bodansky, D. D. Clayton, and W. A. Fowler, Phys. Rev. Letters **20,** 161 (1968); W. D. Arnett, Astrophys. Space Sci. **5,** 180 (1969).

studied in the laboratory,[22,23] but not at quite as low an energy as they are expected to occur at in the stars. One needs an understanding of the physics of the reactions to extrapolate downwards with accuracy, or to evaluate, at least, the uncertainties of the extrapolation. Many other needed charged-particle reactions have not been measured, especially $(\alpha, p)$, $(\alpha, n)$, $(\alpha, \gamma)$, and $(p, \gamma)$ reactions for target nuclei with masses around and above $^{28}$Si. Some of those reactions probably will never be measured since they involve unstable target nuclei. Theoretical determinations of those rates, based on the optical model, have been used by astrophysicists.

In principle, they could have solved the Schrödinger equation of the Woods-Saxon optical model for each channel and for each nucleus. Because of the large number of rates needed, they have relied upon square-well black-nucleus calculations. The accuracy with which the equivalent square well replaces a diffuse well vindicates their efforts, but it also shows the relationship between the radius obtained by fitting scattering data to an optical model and the radius one should use in absorption cross sections. By fitting experimental reaction cross sections for $(n, p)$ reactions (for $37 \leq A_{\text{target}} \leq 60$) and for $(p, \alpha)$, $(p, \gamma)$, and $(\alpha, \gamma)$ reactions (for $A \simeq 35$) to black-nuclei cross sections, Truran *et al.*[24] determined a radius $R = 1.2 (A_0^{1/3} + A_1^{1/3})$ fm, where $A_0$ is the mass number of the projectile and $A_1$ is that of the target. From electron and elastic scattering data, one rather expects $R_0 = 1.25\ A^{1/3}$ fm for protons and neutrons, and $R_0 = 1.09\ A^{1/3} + 1.6$ fm for $\alpha$ particles. From Fig. 9, one should add to obtain the ESW radius $\Delta R = 0.1$ fm for protons and neutrons and $\Delta R = 0.7$ fm for $\alpha$ particles. The radius obtained by Truran *et al.* is seen to be larger than the scattering one for nucleon channels and very nearly the same for $\alpha$ channels. Part of the discrepancy probably comes from the artificial reflection occurring in the black nucleus. If the reflection factor is used to multiply the penetrability, the radius needed to fit the $(n, p)$ reaction measurements is smaller. The $\alpha$-channel radius is also reduced, however. We have made calculations, using diffuse-well transmission functions, of the reactions $^{27}$Al$(p, \alpha)$ $^{24}$Mg and $^{31}$P $(p, \alpha)$ $^{28}$Si. Comparing these with the experimental[25] cross sections points to an $\alpha$-channel radius $R_0 = 1.09A^{1/3} + 1.6 \pm 0.4$ fm, in good agreement with the radius for particle scattering.

It is then possible to relate the parameters to be used in reaction cross-section calculations to those obtained from electron, meson, $p$, $n$, and $^4$He scattering by nuclei. Formulas like Eq. (C-60) of Fowler and Hoyle[26] may be used if one replaces $\beta$ by $f\beta$, that is, if one multiplies the penetrability, or equivalently the strength function, by the reflection factor. The radius to be used is then the one obtained from scattering experiments plus the $\Delta R$, from Fig. 6 or Fig. 9. One can use Eq. (C-60) of Ref. 26 to estimate the uncertainty in the reaction rates caused by the uncertainty in the parameters of the optical model.

Changing the depth $V_0$ of the potential has only a second-order effect: The first-order effects in Eq. (C-60) are due to reflection, and they are cancelled by the dependence of $f$ on $V_0$. The effect of the surface thickness $a$ is more profound. Increasing it by 25% will generally increase the $f$ factor by 25%, but, more important, it will sometimes, as for $^{32}$S+$^4$He, increase $\Delta R$ by a factor of 2 (see Fig. 6). All important uncertainties can then be related to the radius $R_0$ of the diffuse well and to the $\Delta R$ needed to obtain the radius of the ESW. For $^{32}$S+$^4$He at $T = (3.0 \times 10^9)$ °K, it can easily be calculated, using Eq. (C-60), that changing the radius from $R = 5.6$ to $R = 6.6$ fm increases the reaction rate by a factor of 5.0. Uncertainties in the radius and the surface thickness then seem to introduce uncertainties of a factor of 5.0 in the reaction rates involving $^4$He channels.

In the preceding discussion, it was assumed that the optical model is a proper representation of the $^4$He reaction channels. We can also study how sensitive the value of $\langle \sigma v \rangle$ is on the underlying physics. To this end, we have used as our optical potential

$$V(r) = -V_0\{1+\exp[(r-R_0)/a_v]\}^{-1} - iW_0\{1+\exp[(r-R_0)/a_w]\}^{-1}, \quad (44)$$

and we have varied $a_W$ while keeping $a_V$ constant. This represents one of the ways in which the commonly used optical model can be modified to represent different hypotheses as to matter distribution and the location of the compound-nucleus formation.

Numerical calculations have been carried out for $^{32}$S+$\alpha$, $^{44}$Ti+$\alpha$, and $^{12}$C+$^{12}$C with $a_V \neq a_W$. The ratios $T_l(a_W \neq a_V)/T_l$ (ESW) are presented in Fig. 12. Whereas the equivalent square well is a good approximation to the diffuse well for $a_W = a_V$, it breaks down completely if $a_W > a_V$. The cross section is then dominated by absorption in the barrier, as can be seen for $^{12}$C+$^{12}$C in Fig. 13. The low-energy cross section obtained with the black nucleus could then easily be an underestimate by another factor of 5. This is expected to be important, especially for $\alpha$ particles incident on nuclei with large $Z$ $(Z \geq 20)$. However, the data available for $\alpha$-particle channels in reaction cross sections at low energy are for $^{31}$P $(p, \alpha)$ $^{28}$Si, $^{27}$Al $(p, \alpha)$ $^{24}$Mg,

[22] J. R. Patterson, H. Winkler, and C. S. Zaidins, Astrophys. J. **157**, 367 (1969).
[23] J. R. Patterson, H. Winkler, and H. Spinka (private communication).
[24] J. W. Truran, C. J. Hansen, A. G. W. Cameron, and A. Gilbert, Can. J. Phys. **44**, 151 (1966).
[25] P. M. Endt and C. Van der Leun, Nucl. Phys. **A105**, 1 (1967).
[26] W. A. Fowler and F. Hoyle, Astrophys. J. Suppl. **91**, 201 (1964).

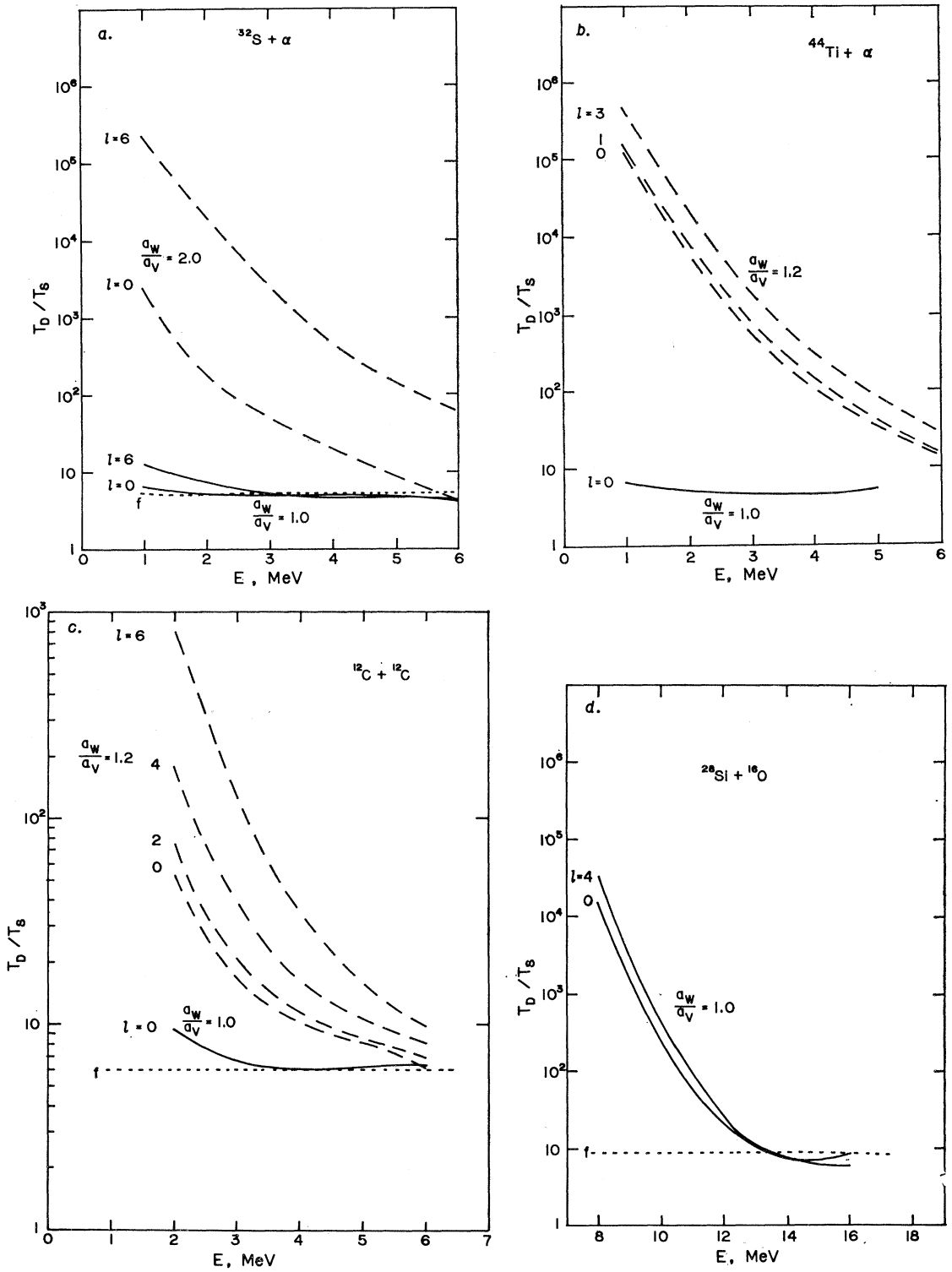


FIG. 12. Ratios of transmission functions for a variety of reactions. Even in the presence of moderate barriers [Fig. 12(a)], the barrier absorption is seen to depend strongly on the surface thickness of the imaginary potential. In fact, even a slight increase in the barrier [Fig. 12(b)] is seen to considerably enhance the barrier absorption. On the other hand, it is rather insensitive to the reduce mass [Fig. 12(c)]. In all these cases, the ESW model is seen to have considerable validity provided we choose a conventional surface thickness for the imaginary potential ($a_W = a_V = 0.5$ fm). In the presence of the extreme barriers associated with heavy-ion reactions and $\alpha$-particle scattering from heavy nuclei [Fig. 12(d)] it is seen that the ESW model fails badly even for conventional surface thicknesses. Hence, it is of crucial interest to understand the details of the imaginary potential in the barrier if one wishes to extrapolate high-energy data to the energies of interest to astrophysics.

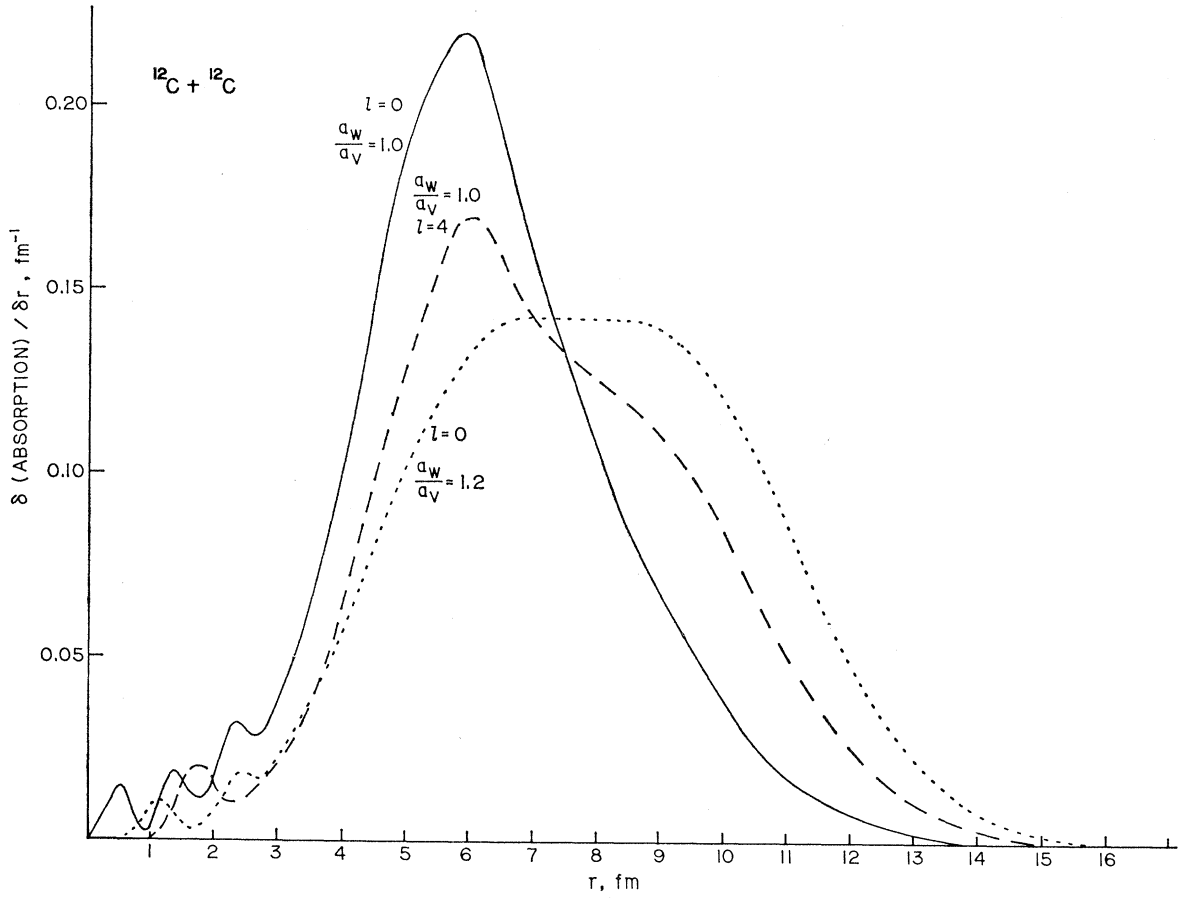


FIG. 13. Fraction of the absorption as a function of the radius for a diffuse potential whose real and imaginary parts have Woods-Saxon shapes with parameters appropriate to the reaction $^{12}C+^{12}C$. The comparison of the absorption for $s$ waves (solid) and $g$ waves (dashed) shows that the relative amount of absorption that occurs in the barrier is increased when the barrier is heightened. It is also seen that increasing the surface thickness $a_W$ of the imaginary potential (dotted) considerably enhances the relative amount of barrier absorption. Hence, low-energy absorption cross sections may yield detailed information about the shape of the absorptive potential in the nuclear surface. (The energy is 4 MeV.)

and $^{35}Cl$ $(p, \alpha)$ $^{32}S$. (Since the $Q$ value of those reactions is positive, the transmission function for protons is approximately equal, at a given energy in the compound nucleus, to that for $\alpha$ particles. The $\alpha$-particle transmission function is reasonably large and is not expected to show absorption in the barrier.) Fitting these with black-nuclei cross sections and then extrapolating to higher mass numbers completely neglects the possibility of absorption in the barrier. More experimental data are needed to permit reliable estimates of $\alpha$-particle channels at $A \gtrsim 40$.

The $^{12}C+^{12}C$ results indicate how sensitive the cross section of the $^{12}C+^{12}C$ reaction is on the detailed shape of the optical model chosen. A 20% increase in the diffuseness parameter of the imaginary potential increases the cross section by a factor of 5 at $E \simeq 3$ MeV. Only a model that would represent closely the physics of the $^{12}C+^{12}C$ system could be hoped to permit any extrapolations. The recent results of Ref. 22 may indicate that the optical model is too crude a tool.

## 7. GENERAL CONCLUSIONS CONCERNING NUCLEAR REACTIONS

Our analysis of the role of the optical potential in barrier penetration suggests a number of general conclusions about nuclear reactions. They concern the role of the radius in resonance reactions, the value of the nuclear radius in reactions, and the use of absorption cross sections far below the barrier to probe the tail of the nuclear-density distribution.

The many-channel theory of resonance reactions appears to have a much more complicated geometry than the one-channel potential-scattering problem whose wave properties we described in Sec. 4. We shall show that it is reasonable to decompose the scattering matrix in a manner such that each reaction channel possesses the one-channel potential-scattering properties. Then we can use our earlier results for the one-channel case to remove many of the artificial square-well aspects of the resonance-theory results. A similar

treatment for nuclear reactions without barriers was given in an earlier paper by Vogt.[12]

The general theory of nuclear reactions[10] provides a framework in which all cross sections can be described in terms of level parameters. The relation between cross sections and level parameters is made in two steps. First, the cross section $\sigma_{cc'}$, for an initial channel $c$ and a final channel $c'$, is written in terms of statistical spin factors and collision-matrix components. Next, the collision-matrix components $U_{cc'}$ are written in terms of level parameters

$$U_{cc'}=\exp[i(\Omega_c+\Omega_{c'})](\delta_{cc'}+i\sum_{\lambda\lambda'}\Gamma_{\lambda_c}{}^{1/2}\Gamma_{\lambda_{c'}}{}^{1/2}A_{\lambda\lambda'}), \quad (45)$$

where the $\Omega_c$ are phase shifts and the $A_{\lambda\lambda'}$ the components of a matrix whose inverse is

$$(A^{-1})_{\lambda\lambda'}=(E_\lambda-E)\delta_{\lambda\lambda'}+\Delta_{\lambda\lambda'}-(i/2)\Gamma_{\lambda\lambda'}. \quad (46)$$

This form of the framework is completely general: It applies to all approximate forms from the Breit-Wigner formula to the Hauser-Feshbach theory. The question is, how do the level parameters change when a reaction channel is assumed to include an average Woods-Saxon potential.

The square-well interaction is easily adapted to the ordinary reaction theories. For a square well, both the partial widths and the level shift can be factored in a manner that separates out the many-body features of the problem and in a manner that clearly displays the wave properties associated with the average interaction:

$$\Gamma_{\lambda_c}=S_{\lambda_c}{}^p\Gamma^{lp}=S_{\lambda_c}{}^p 2P_l(\gamma^{lp})^2, \quad (47)$$

$$\Delta_\lambda=-\sum_c S_{\lambda_c}{}^p S_l(\gamma^{lp})^2. \quad (48)$$

The spectroscopic factors $S_{\lambda_c}{}^p$ are essentially statistical coefficients which measure the probability for finding the compound nucleus in the particular mode specified by the channel number $c$. Since they depend on averages over the nuclear volume, they are insensitive to the details of the nuclear surface. Thus, the effects of the surface influence only the one-body aspects of the problem, the single-particle widths $\Gamma^{lp}$ or the corresponding single-particle reduced widths $(\gamma^{lp})^2$. Therefore, the transition from a square-average interaction to a Woods-Saxon interaction affects only the single-particle width. The single-particle width is affected by the diffuse edge in the manner discussed in Secs. 2 and 3. Thus, the insensitivity of the spectroscopic factors to the precise value of the matching radius makes our wave analysis apply to each reaction channel separately.

The conventional treatment of nuclear reactions by the black-box or resonance theories is essentially a square-well treatment. Because of this fact, the nuclear-radius required in this treatment to fit observed reaction rates was artificially large. For several decades, the usual value of the nuclear radius for nuclear reactions was

$$R=1.4(A_1{}^{1/3}+A_2{}^{1/3})\text{fm}, \quad (49)$$

where $A_1$ is the atomic weight of the target nucleus and $A_2$ that of the bombarding particle. On the other hand, the usual optical-model radius for nucleons is

$$R=1.25A_1{}^{1/3}\text{ fm} \quad (50)$$

and for heavy ions

$$R=1.25(A_1{}^{1/3}+A_2{}^{1/3})\text{ fm} \quad (51)$$

or perhaps

$$R=1.09(A_1{}^{1/3}+A_2{}^{1/3})\text{ fm}. \quad (52)$$

For both nucleons and heavy ions, the difference in the radii is usually between 1 and 2 fm. It is our conclusion that the larger radii were a result of the square-well treatment.

Before embarking on an explanation of the differences between old and new radii, we make some remarks on the current fashions. The charge radii of nuclei, as measured by electron scattering and mesic atoms, are $1.09\times A^{1/3}$ fm. If this is taken to reflect the nuclear density as well as the charge, a nucleon should feel the same radius—the same value should apply to the optical potential. Similarly, 1.09 $(A_1{}^{1/3}+A_2{}^{1/3})$ should then be the radius for heavy-ion reactions. Now, there are some additional effects which tend to increase the optical-model radius slightly and to make it slightly dependent on the shell structure. The first is core polarization—an incoming nucleon pulls the target nucleons toward it. The second is the neutron excess in the surface of a nucleus—an excess that leads to the isotopic-spin term in the optical potential. Such a term means that the density extends beyond the charge. Both of these effects can be estimated only roughly and depend on the particular nucleus involved. Their magnitude roughly justifies the small amount by which current radii exceed the charge radii. There is some experimental uncertainty in the radii as well. Although the wave resonance effects determine the product $V_0R_0{}^2$ very accurately (perhaps to 1%), we know of no experiment that unambiguously determines the radius of the real part of the optical potential to anything like this accuracy. Therefore, the choice for nucleons of $1.25A^{1/3}$ is not only a reasonable choice but also has about a 10% uncertainty. By the same token, an $\alpha$-particle radius of 1.6 is also reasonable.

From our analysis of wave properties, we see that there are several ways in which the change from an optical potential to a square well modifies the radius. First, there is the difference in reflection between the wells, which can be compensated for by a difference in radii; second, there is the wave oscillation in the tail of the real part of the optical potential that leads (Fig. 5) to a difference in radius between the optical potential and its equivalent square well; third, there is absorption in the tail of the imaginary part of the potential.

A reassessment of the old analyses needs to examine only the heavy-ion absorption cross sections for which the dependence on the nuclear radius is unambiguous. For nucleons, it has turned out that there are size-resonance effects which vary through the Periodic Table (see Fig. 2). For $\alpha$ particles and other heavy ions, all the size-resonance effects are washed out, (particles reaching the nucleus are absorbed). Early evidence[27] for the large radius came from charged-particle reactions[27] as well as neutron reactions.

In the black-nucleus model for $\alpha$-particle absorption, the strength function was shown (Sec. 2) to be that of a square well. It has no giant-resonance structure, but neither does the diffuse-edge optical-model potential suitable for $\alpha$-particle reactions. We might therefore be tempted to say that the black-nucleus radius should be chosen to be that of the ESW of the appropriate optical potential. In such a choice, the $\Delta R$ of Fig. 9 has a value of about 0.5 fm. But such a choice ignores wavereflection. From Fig. 9, the reflection factor for $\alpha$ particles has a value between 3 and 5. The transmission functions far below the barrier are directly proportional to the reflection factor. To enhance the black-nucleus transmission functions by a factor of 3 to 5, we can increase the nuclear radius, thus increasing the penetration factor. The required increase in the radius is about 0.5 fm. {The penetration factor at an energy $E$ far below the Coulomb barrier $B$ depends on the nuclear radius roughly as

$$P \cong kRG^{-2}(kR) \propto kR \exp(-2kR),$$

where

$$k=[(2m/\hbar^2)(B-E)]^{1/2}.$$

For $\alpha$ particles, $k$ typically has values between 1.0 and 2.0.} Thus, the wave oscillation ($\Delta R \simeq 0.5$) and the wave reflection together account for the 1.0 fm difference between the black-nucleus radius and that of modern optical potentials. The early analysis of $\alpha$-decay rates in heavy nuclei required similar anomalously large radii that have been brought into agreement with modern values by our wave analysis.[14] In our view, there is no evidence at all that any nuclear reaction rates require anomalously large radii or that they throw into question the individual particle picture of nuclear structure.

The sum-rule limits associated with reduced widths are square-well values that need to be modified to take into account the reflection factor of a diffuse-edge well. According to Eq. (20), for any reaction channel we can write a single-particle width as

$$\Gamma^{lp}=2P_l(\gamma^{lp})^2=2P_lf(\gamma_{\mathrm{SW}}{}^{lp})^2, \tag{53}$$

where $P_l$ is the conventional penetration factor [Eq. (6)] and $(\gamma^{lp})^2$ the single-particle reduced width of the well. Equally, we can write

$$(\gamma^{lp})^2=f(\gamma_{\mathrm{SW}}{}^{lp})^2=f\hbar^2/mR_0^2, \tag{54}$$

where $f$ is the reflection factor discussed above and $(\gamma_{\mathrm{SW}}{}^{lp})^2$ is the single-particle reduced width of the ESW. It is $(\gamma_{\mathrm{SW}}{}^{lp})^2$ that has the conventional sum-rule value of $\hbar^2/mR_0^2$ where $R_0$ is the radius of the ESW. Therefore, a true single-particle level *should* have a reduced width exceeding the conventional sum-rule limit by the reflection factor $f$, which typically has a value between 2 and 5. Our work shows that this factor applies to all charged-particle reactions as well as to neutrons and gives quantitative estimates of $f$.

Far below the barrier, the absorption in the tail of the optical potential can dominate the whole absorption process. We have warned of the dangers of using conventional optical models to calculate reaction rates that are dominated by their tails. We can, however, turn the argument around and suggest that the measurement of absorption cross sections far below the barrier be used to determine nuclear properties at large radii. This is a problem of considerable importance in modern nuclear physics because of fission isomerism,[28] mesonic atoms,[29] and the general question of nuclear clusters in regions of low density. From our study, it is clear that any nuclear density (whether of nucleons or other clusters) extending to large radii can dominate the absorption process. It would be very interesting and valuable to perform nuclear reactions with intense beams at low energies to examine, say, the probability of $\alpha$-particle absorption in the bombardment of many light nuclei. Similarly, experiments with proton or heavy-ion beams might also yield anomalously large cross sections. Is $^{16}$O much more tightly bound than $^{20}$Ne or $^{24}$Mg? Does the distant tail of the nuclear density in the latter present nucleons or $\alpha$-particle clusters? It is likely that the kind of surprises found in the $^{12}$C+$^{12}$C reactions[22] will abound in many other cases. The results may also change many of our notions concerning stellar reaction rates.

---

[27] See, for example, J. P. Blaser, F. Boehm, P. Marmier, and D. C. Peaslee, Phys. Acta **24,** 3 (1951). A complete discussion of early nuclear reactions is found in Blatt and Weisskopf's book, Ref. 3.

[28] V. M. Strutinsky, Nucl. Phys. **A95,** 420 (1967); E. Migneco and J. P. Theobald, *ibid.* **A112,** 603 (1968).

[29] S. Devons and I. Duerdoth, in *Advances in Nuclear Physics,* edited by M. Baranger and E. W. Vogt (Plenum Press, Inc., New York, 1969), Vol. 2, p. 295.